Earth-Science Reviews 136 (2014) 121–140

Contents lists available at ScienceDirect

Earth-Science Reviews

journal homepage: www.elsevier.com/locate/earscirev

Controls on erosion intensity in the Yangtze River basin tracked by U–Pb detrital zircon dating

Mengying He [a], Hongbo Zheng [b,*], Bodo Bookhagen [c], Peter D. Clift [d]

[a] School of Earth Sciences and Engineering, Nanjing University, Nanjing 210023, China
[b] School of Geography Science, Nanjing Normal University, Nanjing 210046, China
[c] Geography Department, University of California, Santa Barbara, Santa Barbara CA 93106-4060, USA
[d] Department of Geology and Geophysics, Louisiana State University, Baton Rouge, LA 70803, USA

ARTICLE INFO

Article history:
Received 21 May 2013
Accepted 20 May 2014
Available online 29 May 2014

Keywords:
Yangtze River
Sediments
Detrital zircons
Erosion
Provenance
Stream power

ABSTRACT

The Yangtze River dominates the drainage of eastern Asia, yet the processes that control erosion within the basin are obscure, making the interpretation of the detritus record difficult. In this study we used U–Pb dating of zircon grains from the modern main stream and major tributaries to identify the sources of sediment production, based on the diversity of zircon ages associated with the different tectonic blocks over which the Yangtze flows. We demonstrate that tributaries in the central part of the catchment are the most important in supplying sand-sized sediment to the main stream, i.e., the Hanjiang, Xiangjiang and Jialingjiang, as well as along the main stream (Jinshajiang) between Panzhihua and Yibin. Surprisingly, the rivers draining the eastern edge of the Tibetan plateau do not appear to dominate the modern budget, despite their tectonic activity and steep topography. Sediment-productive drainages have high specific stream power (because of significant rainfall as well as steep topography), but are also the locations of early human settlement and agriculture. We suggest that it is the combination of high specific stream power and anthropogenic disruption to the landscape that facilitates sediment supply to the main stream. Because of zircon transport times spanning thousands of years reworking during early to late Neolithic settlement, may be more important than recent farming in controlling the zircon population of the river sands. Our sediment-transport framework explains the discrepancy between sediment sources identified by zircon dating and the strong sediment production in the upper reaches favored by studies of fine-grained sediment or cosmogenic isotopes applied to quartz grains.

Contents

* Corresponding author at: School of Geography Science, Nanjing Normal University, 1 Wenyuan Road, Nanjing 210046, China. Tel.: +86 25 85891259.
E-mail address: zhenghb@njnu.edu.cn (H. Zheng).

http://dx.doi.org/10.1016/j.earscirev.2014.05.014
0012-8252/

1. Introduction

Erosion and sediment-mass transport is an integral part of the process of recycling of continental crust. Rocks are eroded from mountain belts into sedimentary deposits on continental margins where they may be involved again in the plate tectonic cycle as that ocean basin closes to form another generation of mountains. Erosion is a fundamental process in shaping planet Earth, as well as playing a role in controlling global sea-level and average crustal thicknesses (Whitehead and Clift, 2009). Erosion is moreover a fundamental step in driving chemical weathering, which has been argued to be an important control on global climate through the drawdown of CO_2 in the atmosphere (Raymo and Ruddiman, 1992; Berner and Berner, 1997).

If we are to understand how topography has evolved and what controls erosion we must first understand river systems and how they derive sediment from the landscape and deliver it to the ocean. In this study we examine how erosion varies across the Yangtze River basin (1.8×10^6 km^2) of central China (Fig. 1A). The Yangtze is a suitable place to examine the processes of continental erosion because there is a large sediment load in this river, ~480 Mt/yr prior to human disturbance (Milliman and Syvitski, 1992), and the basin itself is subject to strong forcing both through tectonic activity, steep landscapes and a seasonal climate. The western part of the Yangtze basin covers the eastern portion of the Tibetan Plateau, the highest plateau on Earth and one of strong, active rock deformation (Zhang, 2013). Furthermore, the region is influenced by the summer rains of the Asian monsoon, which is itself partly controlled by the growth of topography in High Asia (Prell and Kutzbach, 1992; Molnar et al., 1993; Huber and Goldner, 2012).

The western, high-elevation part of the Yangtze basin tends to be dry, with more rain toward the east, although we recognize that areas of stronger precipitation related to orographic rainfall over steep slopes also exist in locations such as the Sichuan Basin. The strong heterogeneity in tectonic activity and in rainfall are two of the reasons why erosion may not be uniform across the Yangtze basin. In this paper we use the changing zircon populations in the main stream of the Yangtze, as well as in the major tributaries to determine where the zircon grains are being contributed to the net flow in large numbers, a method that depends on the heterogeneity in the zircon age populations of the bedrock sources across the drainage. In doing so we reveal how sediment production varies spatially so that we can then compare patterns of relative erosion intensity between tributary basins with the different possible forcing processes to understand which of these is dominant in generating sediment. Only through understanding where the sediment is coming from within a large river basin are we able to interpret sedimentary basin and marine sedimentary records in terms of evolving mountain building, or changing climate onshore.

2. Previous studies

Some data already exist that help us understand the provenance of sediment in the Yangtze River. Regional sampling of the clay minerals within the Yangtze indicates that the northern, central parts of the drainage provide the bulk of the fine-grained sediment in the river (He et al., 2013b). This result is consistent with Ar–Ar dating of muscovite sand grains from the First Bend and the river mouth that indicate little influence from the Jinshajiang and apparent dominance of sources north of the Sichuan Basin (Hoang et al., 2010) (Fig. 1A). However, muscovite grains are fragile and can be broken during transport so that it is unclear if the lack of micas from the upper reaches within sands from the delta really represents a low supply from that region or simply reflects the destruction of these grains during transport (Garzanti et al., 2009). We further note that both clay and muscovite are low-density minerals, often transported in the suspended load. Consequently, these data tell us little about the source of the sand and bedload, which may be composed of generally denser minerals, such as zircon. Study of the Red River showed that zircon and mica provenance budgets are not always in agreement, reflecting the slower transport of zircon, different resistance to physical abrasion and chemical weathering, because of the distinctively different shapes of mica and zircons, and because of changing erosion patterns (Hoang et al., 2010).

Studies have also been performed on sand-sized grains based on the major element chemistry and ^{10}Be cosmogenic isotopes in quartz-dominated sand (Chappell et al., 2006). That study suggested that ~65% of the quartz sand material reaching the ocean is derived from the western parts of the drainage, including the Sichuan Basin, in agreement with heavy mineral studies that show more sediment production in the upper reaches (Yang et al., 2009). Quartz has a much lower density than zircon and is expected to travel more quickly from source to sink. This and the different time scales of processes producing cosmogenic isotopes imply that the Chappell et al. (2006) study provides a better image of the more recent erosion patterns in the Yangtze Basin than one focused on zircon. Zircon budgeting need not agree with the result of heavy mineral studies because zircon is only one minor part of that entire assemblage and travels more slowly to the delta. Chemical weathering in the lower reaches is effective at reducing the concentration of mafic heavy minerals, so that it is not surprising that the upper reaches would be relatively rich in these phases.

In our study we target zircon grains in the Yangtze. Zircon is substantially denser and chemical resistant and also has potentially long transport times. 5000–10,000 yr was estimated in the Indus River for the recent past (Clift and Giosan, 2014), which is approximately half the length of the Yangtze, 3200 km versus 6300 km, so that transport times in the lower reaches may be even longer and likely spans at least thousands of years. This means that zircon provenance work may reflect paleo-erosion patterns that took place under different climatic conditions and with different patterns and intensity of human settlement. This approach is less likely to be affected by 20th century damming of the river, which has an immediate impact on the faster moving mineral species.

3. Geologic and geographic setting

The Yangtze River originates from the Tibetan Plateau at an elevation higher than 5000 m, and reaches the East China Sea after flowing more than 6300 km. The Yangtze has a catchment area of 1.8×10^6 km^2 and an annual average discharge of $\sim 9.0 \times 10^{11}$ m^3, based on long-term (1950–2000) hydrologic observations (Chen et al., 2001; Ding et al., 2004; Yang et al., 2004a). The river catchment can be divided into five broad physiographic provinces, including the northeast Tibetan Plateau, the high mountains of the Longmen Shan and associated ranges, the Sichuan Basin, mixed mountain and basin terrains (broadly referred to as the Three Gorges area), and the eastern lowlands (He et al., 2013b) (Fig. 1A). Conventionally, the basin is divided into three parts, the upper, middle and lower reaches. Geographically, the upstream can be divided into two segments, the Jinshajiang segment and the Chuanjiang segment (Fig. 1A).

The Yangtze River drainage covers several tectonic units, including the Qamdo Block, the Songpan–Garze terrane, the Qinling–Dabie orogenic belts and the South China Block, which is composed of the Yangtze Craton and the Cathaysia Block. The Yangtze Craton underlies the main part of the Yangtze River drainage (Fig. 2A). The relative proportions of different zircon age groups in the bedrock of the different tectonic blocks drained by the Yangtze River are displayed in Fig. 2B. This allows us to see the major tributaries and the corresponding tectonic units, which ultimately affect the zircon age population in each stream.

The Qamdo Block located in the west of the drainage, experienced five evolutionary phases, which are the formation of Precambrian crystalline basement and the Early Paleozoic fold basement, the development of a volcanic arc to back-arc basin setting in the Late Paleozoic, the formation of a foreland basin during the Triassic and the evolution of a strike-slip pull–apart basin in the Cenozoic (Du et al., 1997). The

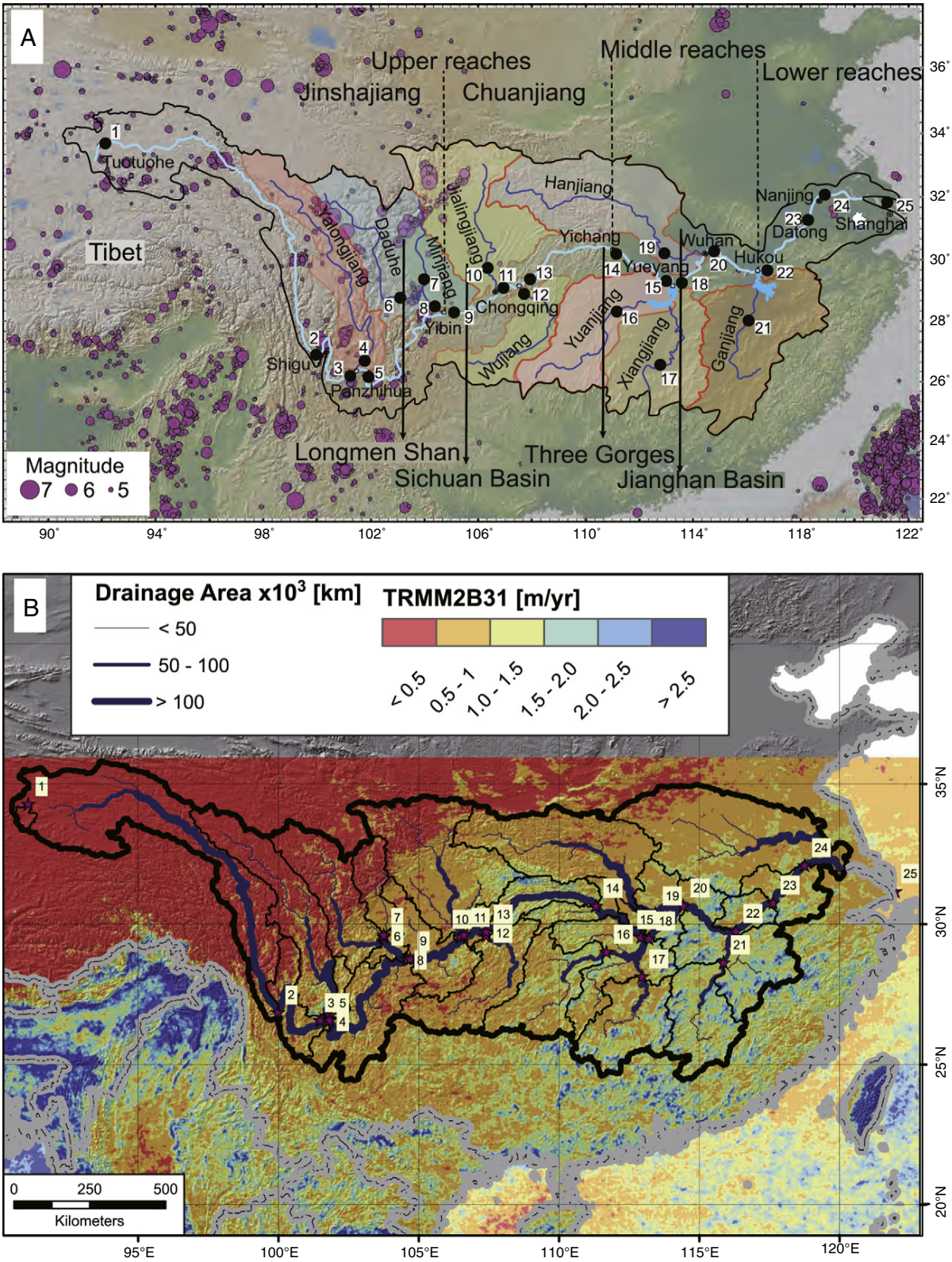

Fig. 1. (A) Shaded topographic map showing the major tributaries, the sample locations and the earthquake locations within the Yangtze drainage basin. Topography is from the Shuttle Radar Topography Mission (SRTM) and earthquake data are from US Geological Survey and National Earthquake Information Center (Ryan et al., 2009), scaled by magnitude >5.0. Numbers refer to samples that are shown in other figures in this paper. (B) Average annual precipitation for the Yangtze River Basin calculated from calibrated, satellite-derived rainfall (product TRMM 2B31, see (Bookhagen and Burbank, 2010) for processing details). Numbered boxes relate to sample locations.

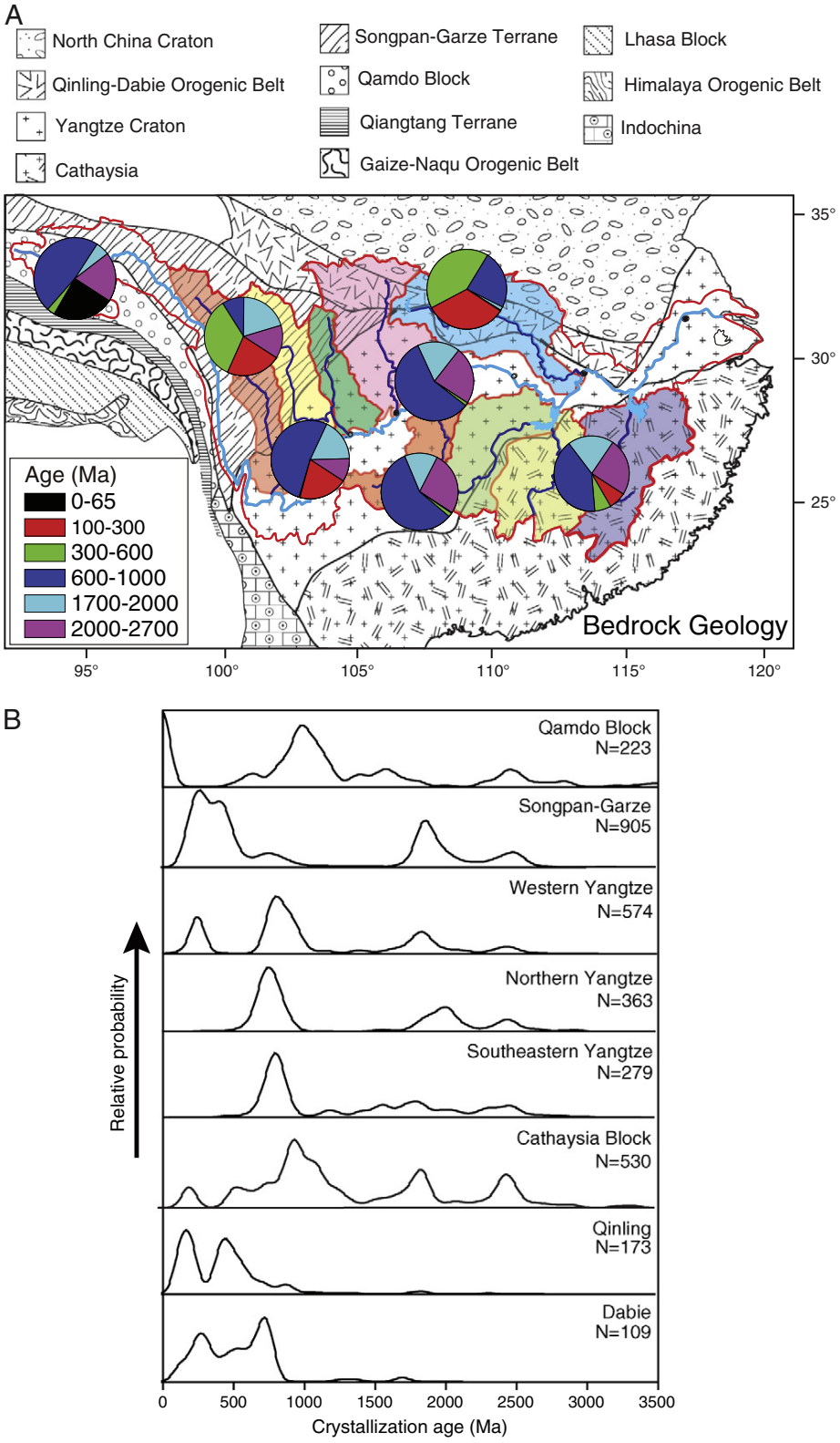

Fig. 2. (A) Tectonic map of central China and pie charts of published zircon U–Pb ages showing the major structural blocks and in color the catchment of the major Yangtze tributaries in order to show the potential provenance of the sediments in each of those basins. Map is altered after (Pubellier et al., 2008). (B) Kernel Density Estimation (KDE) plots for the zircon U–Pb ages of geological units. Data from the Qamdo block is from (Wei et al., 2007; Wu et al., 2007; He et al., 2013d). Data from the Songpan Garze is from (Hu et al., 2005; Weislogel et al., 2006). Data from the western Yangtze Block are from (Sun et al., 2009) and (Xu et al., 2008). Data from the northern Yangtze Block is from (Wang et al., 2012). Data from the southeastern Yangtze Block is from (Wang et al., 2010). Data from the Cathaysia Block is from (Yao et al., 2011; Xia et al., 2012). Data from the Qinling–Dabie orogenic belt are from (Zhao et al., 2008; Qin et al., 2009; Wang et al., 2009; Li et al., 2012).

Qamdo Block exposes Cretaceous–Cenozoic granite in the northwest (Wei et al., 2007; Wu et al., 2007; Jia et al., 2010). The detrital zircon U–Pb dating in biotite plagioclase gneiss from the block exhibit four major ranges, which are 2600–2300 Ma, 1700–1400 Ma, 1200–850 Ma and 700–530 Ma (He et al., 2013d) (Fig. 2B). Recent work by Fei et al. (2013) demonstrated that the Miocene rocks of the Qamdo Block has similar ages to those found in the Songpan–Garze terrane and to the 229–245 Ma ages from the Triassic Yidun volcanic arc, which is located in the north of the Qamdo Block (Reid et al., 2007).

The Songpan–Garze terrane lies in the northwest of the Yangtze catchment. It is bounded by the Yangtze Craton, as well as the North China and the Qamdo continental blocks (Chen and Wilson, 1996). This unit is a folded Triassic flysch sedimentary basin, interpreted as an accretionary complex formed during the closure of a remnant Paleotethyan oceanic basin (Zhou and Garanham, 1993; Weislogel et al., 2006). The terrane basement was a stable block before the Paleozoic. Carbonate rocks were deposited during the Carboniferous. In the Early Permian, the Songpan–Garze terrane was covered by a large area of mafic volcanic rock, linked to the Emeishan Basalts in the western Yangtze Craton (Chung and Jahn, 1995; Bruguier et al., 1997). The Songpan–Garze terrane was affected by the Indosinian orogeny in the Middle Triassic (Carter and Clift, 2008), during which the flysch was deposited (Xu et al., 1992). Following the closure of Paleotethys, the Songpan–Garze terrane was influenced by formation of the Longmen Shan during the Cenozoic (Lan et al., 2006; Zhang et al., 2006). The granite rock ages within the Songpan–Garze terrane are mainly Late Triassic–Earth Jurassic, and the detrital zircon ages have four age populations: 250–280 Ma, 400–450 Ma, 1850–1950 Ma and 2400–2500 Ma (Hu et al., 2005; Weislogel et al., 2006; He et al., 2013c) (Fig. 2B).

The Qinling–Dabie orogenic belt lies to the north of the Yangtze Craton. Meso-Neoproterozoic orogeny mostly affected this belt, followed by a Late Paleozoic marine transgression from the direction of the Songpan–Garze terrane. The belt was strongly affected by orogenic and magmatic events during the Mesozoic to Cenozoic, especially the Triassic Indosinian Orogeny (Liu and Zhang, 1999; Zhang et al., 2004; Carter and Clift, 2008). The major age populations in the Qinling dated to 205–323 Ma and 400–505 Ma, and zircon U–Pb dating in Dabie provides consistent ages of 751 Ma for protolith crystallization, and 213–245 Ma and 126–131 Ma for regional metamorphism (Zhao et al., 2008) (Fig. 2B).

Basement rocks of the Yangtze Craton are rarely exposed. The only known Archean basement rocks are the Kongling Complex in the northern part of the Yangtze Craton (Gao et al., 1999). Although Archean detrital zircon grains have been reported from the Cathaysia Block, which is in the southeast of the drainage, no Archean rock has been identified so far. The oldest crystalline rocks in the Cathaysia Block are 1.9–1.8 Ga granites (Hu et al., 1991; Gan et al., 1995). Most researchers now accept that the Yangtze Craton and Cathaysia Block were joined together by late Neoproterozoic times (Wang et al., 2007; Li et al., 2008; Li et al., 2009). Neoproterozoic igneous rocks ranging in age from 740 to 1000 Ma are widespread in South China. The Western Yangtze Craton also comprises rocks with zircon ages of ~260 Ma, which are regarded as being related with the Emeishan basalt. There are five age populations in the Cathaysia Block: 2560–2380 Ma, 1930–1520 Ma, 1300–900 Ma, 850–530 Ma and 269–220 Ma (Wan et al., 2007; Yao et al., 2011) (Fig. 2B).

Zircons can be divided into a number of naturally clustering age populations that reflect the tectonic evolution of East Asia. We particularly note grains dating at <65 Ma, 100–300 Ma, 300–600 Ma, 600–1000 Ma, 1700–2000 Ma, 2400–2700 Ma, and 3000–3200 Ma. Although grains from many of these groups are found in most tributary basins the relative balance of the populations changes from tributary to tributary because of the different geology in each basin.

The Yangtze River basin consists of diverse rock compositions and strata, including widely distributed carbonate rock, sandstone, volcanic rocks and gneiss dating from the Archean to the Quaternary (Fig. S1). It is recognized that zircons are more abundant in acidic magmatic rocks, siliciclastic sedimentary rocks and their metamorphosed equivalents, while they are absent from carbonate sedimentary rocks and are only sparsely found in mafic magmatic rocks. The changing geology along the main stream and within the major tributaries result in distinct source rock types. In the upper basin, the drainage consists of Mesozoic rocks with subordinate upper Paleozoic and Cenozoic rocks. The eastern Tibetan Plateau is mainly composed of clastic sedimentary rocks, as well as lesser amounts of carbonate and igneous rock, especially Cenozoic intermediate-acid intrusive igneous rocks. The middle–lower basins mostly consist of Paleozoic marine and the Quaternary fluvio-lacustrine sedimentary rocks, together with intermediate–felsic igneous rocks, and older metamorphic rocks (Fig. S1).

The Yangtze catchment is located in the humid sub-tropical climate zone, dominated by the Asian monsoon system, with seasonal alternation between the warm and wet summer monsoon, and the cold and dry winter monsoon. However, there are differences in the patterns of monsoon precipitation between the upper and middle/lower streams (Fig. 1B; Bookhagen and Burbank (2010)). Annual precipitation tends to decrease westward from more than 2000 mm in the eastern lowlands to about 700 mm in the Sichuan Basin, and less than 400 mm in eastern Tibet (Yang et al., 2004b).

4. Samples and methods

We collected 25 sand samples from the Yangtze River drainage during seasons of low river levels in 2008 and 2009. The sampling sites include 15 locations along the main stream and 10 from the major tributaries, covering the whole drainage (Fig. 1A, Table 1). Samples were taken from deposits within the channel such as mid-channel bars, lateral bars and point bars. Most of our riverbed samples were mixtures of sub-samples taken from several points around each sampling site in an attempt to get representative material from the channel at each point. We collected samples near the confluence between the trunk stream and tributaries, two samples in the mainstream above and below the confluence and one in the tributary, avoiding cities, dams and other sources of possible contamination.

Zircons were extracted from the bulk sediments by conventional heavy liquid and magnetic separation techniques, >1000 zircon grains were picked out from each sample and about 200 grains for each were

Table 1
Geographic locations of surface sediments in the Yangtze River drainage basin.

No.	Sample	Longitude	Latitude
1	Tuotuohe	91°5′9.20″	34°17′43.30″
2	Shigu	99°58′52.00″	26°52′14.00″
3	Panzhihua-1	101°29′25.80″	26°35′16.20″
4	Yalongjiang	101°49′16.20″	26°46′2.40″
5	Panzhihua-2	101°49′13.80″	26°35′28.80″
6	Daduhe	103°45′42.00″	29°33′16.00″
7	Minjiang-1	103°45′18.00″	29°37′28.00″
8	Minjiang-2	104°35′9.00″	28°47′4.80″
9	Yibin	104°41′26.40″	28°47′0.00″
10	Jialingjiang	106°29′1.80″	29°33′22.80″
11	Chongqing	106°37′0.60″	29°37′11.40″
12	Wujiang	107°23′33.80″	29°36′20.80″
13	Fuling	107°24′37.20″	29°44′8.40″
14	Yichang	111°18′43.70″	30°39′49.50″
15	Yueyang-1	112°55′7.60″	29°32′49.50″
16	Yuanjiang	111°41′11.20″	29° 1′25.90″
17	Xiangjiang	112°56′55.20″	28° 8′51.60″
18	Yueyang-2	113°11′27.30″	29°29′28.50″
19	Hanjiang	113°25′57.80″	30°23′33.50″
20	Wuhan	114°25′32.90″	30°40′19.10″
21	Ganjiang	115°51′21.50″	28°38′57.90″
22	Hukou	116°18′26.80″	29°46′3.10″
23	Datong	117°37′41.20″	30°46′26.60″
24	Nanjing	118°44′40.10″	32° 6′47.40″
25	Changxing Island	121°58′45.00″	31°11′16.00″

randomly selected under a binocular microscope. The grains were then mounted in epoxy disks and polished to expose their cores. The mounts were photographed in transmitted and reflected light in order to identify grains for analysis. In order to determine the internal structures of zircons and to identify the potential target sites for U–Pb dating, cathode-luminescence (CL) images were acquired by a Mono CL3 + (Gatan, U.S.A.) attached to a scanning electron microscope (Quanta 400 FEG) at the State Key Laboratory of Continental Dynamics, Northwest University, Xi'an. U–Pb dating analyses were performed on polished grain mounts by laser ablation-inductively coupled plasma mass spectrometry (LA-ICP-MS) at the State Key Laboratory of Mineral Deposits Research, Nanjing University, China, using an Agilent 7500a ICP-MS coupled to a New Wave 213 nm laser ablation system with an in-house sample cell. A spot size of 18–25 μm and a 5 Hz repetition rate were used for analyses. All U–Th–Pb isotope measurements were calibrated by using zircon standard GJ-1, with a $^{206}Pb/^{238}U$ age of 601 ± 12 Ma. Accuracy was controlled by the zircon "Mud Tank" standard with an age of 735 ± 12 Ma (Black and Gulson, 1978). The U–Th–Pb method and data acquisition parameters are given by Jackson et al. (2004) and Griffin et al. (2004). Isotopic ratios were calculated by using GLITTER (ver 4.0) with the common Pb correction carried out following the method of Andersen (2002). The age calculations and plotting of concordia diagrams were performed by using Isoplot (ver 3.0) (Ludwig, 2003). We follow the convention of Compston et al. (1992) in using $^{206}Pb/^{238}U$ ages for zircons younger than 1.0 Ga and $^{207}Pb/^{206}Pb$ ages for grains older than 1.0 Ga. We further filtered our data to use only dates from zircons older than 1 Ga that are <10% discordant and <20% for grains younger than 1 Ga. A sample set of around 100 grains is considered generally a minimum for characterizing sand eroded from a geologically complicated drainage basin (Vermeesch, 2004).

5. Results

The U–Pb ages from each of the considered samples were published by He et al. (2013a) and one sample is also shown in Table S1. The spectrum of grain cooling ages are displayed by using the Kernel Density Estimation (KDE) method of Vermeesch (2012), which plots the detrital ages as a set of Gaussian distributions, but does not explicitly take into account the analytical uncertainties. Vermeesch argues that this is a more statistically robust method than probability density plots for identifying the relative abundance of detrital ages when the number of grains and analytical precision are both high. This method allows the age ranges and abundances of the different age populations to be graphically assessed and different samples are more easily compared.

The overall age patterns for main stream and major tributaries are plotted in Figs. 3 and 4. The range of ages seen in the zircon sand grains is remarkably consistent throughout the samples analyzed in that the same age groups are found in many of the samples. In particular, we see a grouping of grains younger than 65 Ma, 100–300 Ma, 300–600 Ma, 600–1000 Ma, 1700–2000 Ma and 2400–2700 Ma, as well as a rare group dating at 3000–3200 Ma. Most of the zircon sand grains dated fall within one of these age ranges.

Within the main stream, there is evolution in the relative abundance of these different groups going downstream. At Tuotuohe (#1), at the river's origin, the youngest group is relatively abundant (17%; Table 2) although there are zircons from all the groups present even in this uppermost part of the river. Going downstream we see a clear change between Shigu (#2) and Panzhihua-1 (#3) where there is a significant decrease in the abundance of grains younger than 500 Ma and a marked increase in the population dating at 1700–2000 Ma (Fig. 3, Table 2). Grains younger than 200 Ma form an insignificant part of the load downstream of Panzhihua-2 (#5). At Yibin (#9) there is also a significant change in that the proportion of the youngest three groups reduces further, while the abundance of 600–1000 Ma grains increases to a maximum (48%). We also see a sharp decrease in the relative abundance of 1700–2000 Ma at this point in the stream (3%). However, downstream of Yibin (#9) the proportion of 1700–2000 Ma grains increases and grains dating at 400–500 Ma almost disappear entirely. There is also a minority population within the range 2400–2600 Ma, accounting for 3% at Yibin (#9) and 6% at Chongqing (#11; Fig. 3).

Downstream of Yueyang (#15,18) there is a progressive increase in the proportion of grains dating at 100–300 Ma and at 600–1000 Ma. The sample from Yueyang-2 (#18) shows a very prominent peak at 400–500 Ma, although this is lost going downstream as a result of dilution by new sediment. 400–500 Ma grains are visible as a significant minority population at Nanjing (#24), but are insignificant by the time the river reaches the ocean. The lower half of the stream is relatively stable compared to the upper reaches and there is especially little change downstream of Hukou (#22). The stability of the age spectrum suggests that not much new sediment joins the river downstream of this point, or that if sediment is being sourced to the river then this is of a composition that is indistinguishable from that delivered from further upstream, and is likely reworked from the flood plains.

The tributaries show significant variability between each other, reflecting the changing nature of the bedrock. In the Yalongjiang (#4) we see a strong dominance of zircon dating at around 780 Ma (Fig. 4), which is a common peak found throughout the tributaries, although it is weak in the Xiangjiang (#17) and the Ganjiang (#21). None of the tributaries show significant numbers of grains younger than 200 Ma. However, all the tributary samples have grains dating 100–300 Ma, although these are relatively scarce in the Yalongjiang (#4) (13%), Wujiang (#12) (7%), and Yuanjiang (#16) (13%) (Fig. 4, Table 2). Grains dating at 400–500 Ma are particularly abundant in the Xiangjiang (#17), Hanjiang (#19) and in the Ganjiang (#21) but are otherwise relatively rare within the system. Grains dating at 1700–2000 Ma are very abundant within the Jialingjiang (#10) (24%) and in the Wujiang (#12) (34%), despite being only a small minority in most of the other tributaries (Table 2). The oldest significant age population (2400–2700 Ma) is also common in the Jialingjiang (#10) (19%) and in the Wujiang (#12) (26%), as well as forming a significant minority in the Yuanjiang (#16) (23%). Significant differences between the major tributaries mean that their addition to the mainstream should make a significant difference to the bulk composition of the river sediment if the input from each tributary is volumetrically important.

It is our ability to identify mixing between the main stream and the different tributaries based on the unique character of zircon U–Pb age population of each tributary that allows us to gauge the relative influence of each tributary in controlling the total flux of sediment into the Yangtze. Because the range of zircon crystallization ages is different in each stream the impact of that tributary on the net flux can be resolved by seeing how the combined flow changes downstream of each confluence.

6. Discussion

6.1. Zircon bedrock ages

We now compare the age of the zircons in the rivers with those in the potential source rocks in order to identify which ones dominate and thus what controls erosion. We consider a number of possible controlling processes but cannot readily address all possible influences, including the role of particles in channel incision, changes in channel width, and storminess (or precipitation intensity rather than just mean annual estimates). Care needs to be taken when comparing bedrock and detrital age data because recent work by Yang et al. (2012) based on analysis of floodplain sediments from the mainstream and ten major tributaries of the Yangtze River revealed that younger zircons were larger or more variable in size than the older grains, indicating the potential influence of hydrodynamic fractionation on zircon size and age. No specific grain size information was collected as part of this study but sand grains larger than 50 μm across and usually less than 150 μm dominated the data set. Yang et al. (2012) concluded that the

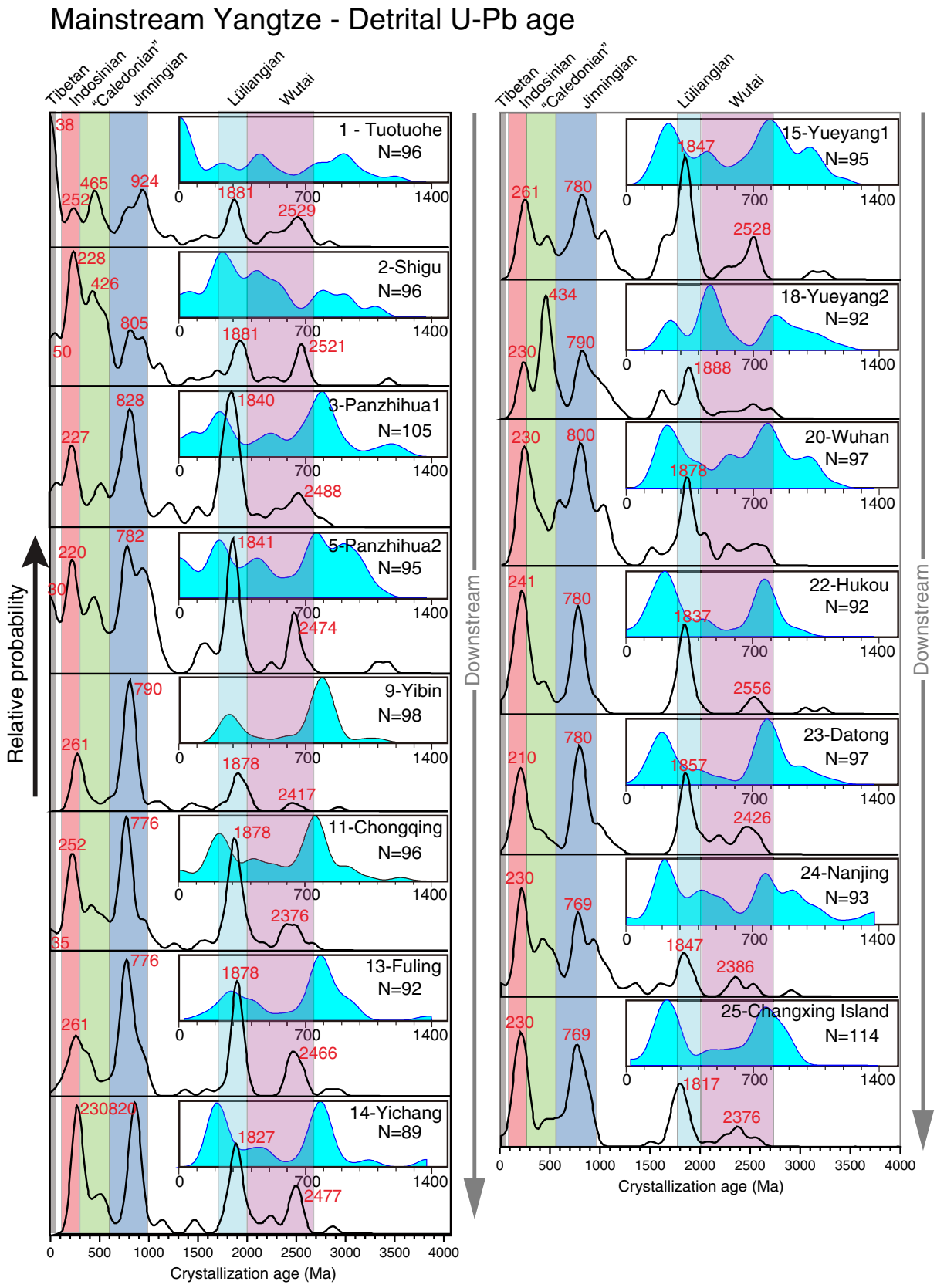

Fig. 3. Kernel Density Estimation (KDE) plots for the zircon U–Pb ages of sands from the main Yangtze River channel. We also show the age spectrum with the narrow range of 0–1400 Ma. The red numbers are the age peak of each group. See Fig. 1A for locations.

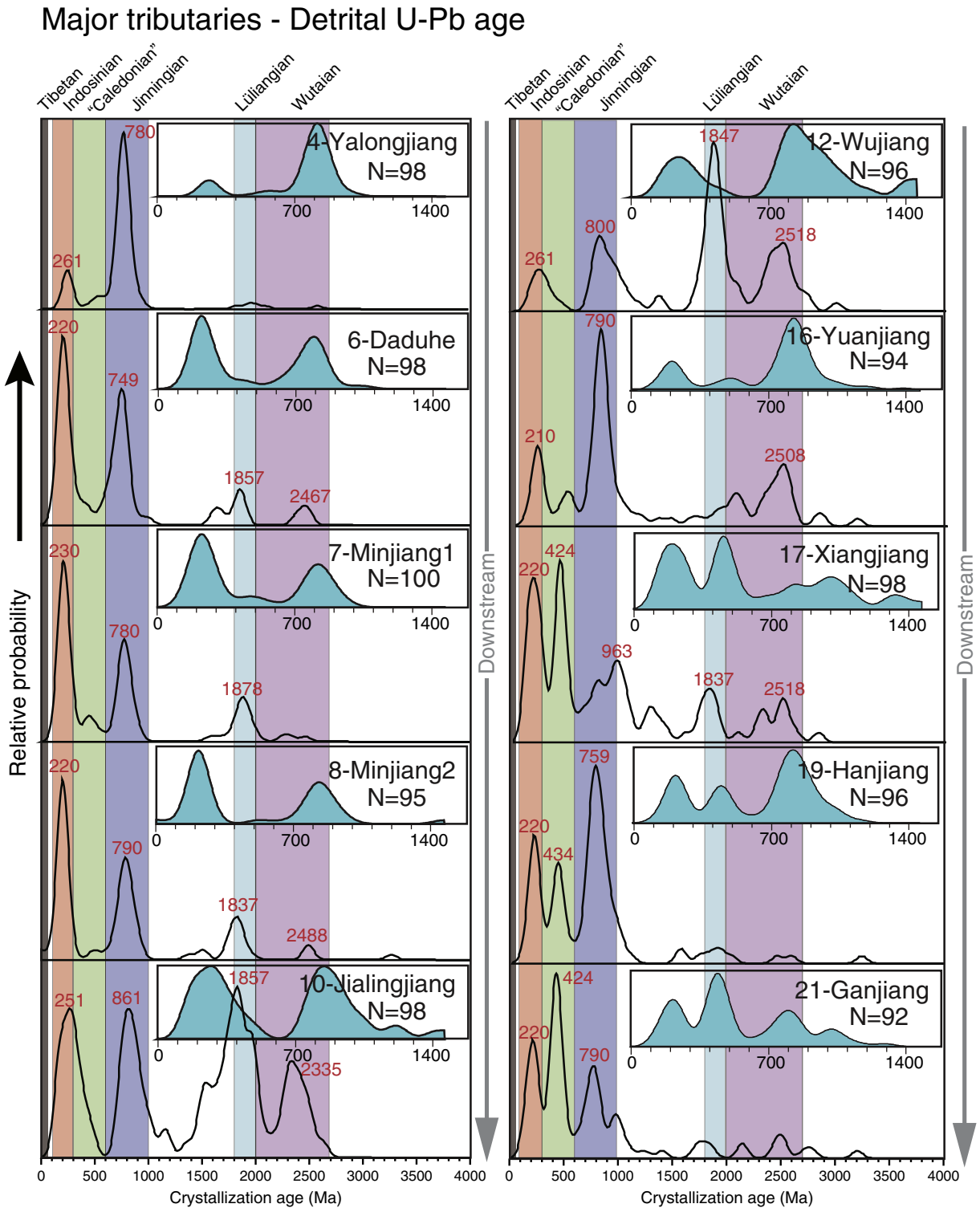

Fig. 4. Kernel Density Estimation (KDE) plots for the zircon U–Pb ages of sands from the tributaries of Yangtze River, as analyzed in this study, also the age spectrum with the narrow range of 0–1400 Ma. The red numbers are the age peak of each group. See Fig. 1A for locations.

63–125 μm size fraction yielded almost the same age population as the bulk population of zircons. As a result our analyses are broadly representative of the total flux in the river. Grains smaller than 50 μm are not readily analyzed using the LA-ICP-MS method and the size of grains considered in this study is generally consistent from sample to sample and we argue that we can exclude grain size as a bias in our conclusions.

Fig. 2A shows that there is a clear heterogeneity in the age of zircon crystallization across the Yangtze basin. The youngest grains dominate those terrains in the upper part of the catchment, in particular the

Table 2
Percentage of zircon age groups in the mainstream and tributaries.

	0–65	100–300	300–600	600–1000	1700–2000	2000–2700
	Ma	Ma	Ma	Ma	Ma	Ma
Tuotuohe	17	8	17	20	13	15
Shigu	5	21	28	18	9	8
Panzhihua-1	2	13	9	25	28	12
Panzhihua-2	4	14	13	28	17	8
Yibin	0	16	8	48	17	3
Chongqing	2	18	11	30	24	10
Fuling	0	11	11	37	24	12
Yichang	0	22	10	27	20	15
Yueyang-1	0	14	11	23	24	11
Yueyang-2	0	11	30	23	14	9
Wuhan	0	16	16	29	14	13
Huhou	1	32	9	28	22	5
Datong	0	19	9	31	19	18
Nanjing	1	20	20	28	11	6
Changxing	1	29	8	34	17	9
Yalongjiang	0	13	5	77	3	2
Daduhe	0	39	8	36	8	5
Minjiang-1	0	43	8	30	12	4
Minjiang-2	1	42	2	34	14	3
Jialingjiang	0	13	9	19	24	19
Wujiang	0	7	3	20	34	26
Yuanjiang	0	13	7	41	5	23
Xiangjiang	0	26	21	20	9	11
Hanjiang	0	21	18	48	4	3
Ganjiang	0	22	34	25	4	7

Qamdo Block, almost 30% of which is composed of grains younger than 65 Ma, while the neighboring Songpan–Garze does not have a significant population from the Cenozoic, but is dominated by 100–300 Ma and 300–600 Ma grains. Zircons of 100–300 Ma age also represent about one quarter of the bedrock within the Western Yangtze Craton itself and almost half of the bedrock within the Qinling–Dabie Orogenic Belt. Bedrock generally becomes older from west to east with the oldest zircons being relatively abundant in the Southeast of the Yangtze Craton (Fig. 2A). The Cathaysia Block is particularly noteworthy in comprising more than 50% grains that are older than 1700 Ma and between 600 and 1000 Ma. Within the Yangtze Craton itself we see a significant change from the west where around one quarter of the total zircon population dates at 100–300 Ma to the northeast where older grains are much more abundant. In that area and in the central southern part of the craton we see that ~35–40% of the total population is older than 1700 Ma.

Our compilation of existing bedrock zircon data (Fig. 2B) explains why the range of ages seen in the modern river sediments changes across the drainage from the headwaters to the river mouth as it receives sediment from different aged source rocks. It is important to note that, although each of the tectonic blocks has a unique signature in terms of zircon age populations, within a given block there are no unique single grain ages, with the possible exception of there being grains <65 Ma present only in significant numbers within the Qamdo Block. Even in the case of grains that are younger than 65 Ma we note that there are Miocene volcanic rocks in the lower reaches of the river (Ma and Wu, 1987), so that although it is statistically more likely that zircons of this age were derived from Tibet it is impossible to exclude the possibility that they were eroded from other parts of the river basin. In theory, for example, a zircon dating at 100–300 Ma could be derived from many of the potential source blocks. We are able to limit the provenance of a particular sand based on the relative abundance of the different age populations rather than relying on a single age assignment to tie a single grain to one source block.

6.2. Detrital zircon ages

In Fig. 5 we show some of the variability in the overall character of the zircon population, which was shown in the form of KDE plots in Figs. 3 and 4. In Fig. 5 we have recalculated the total population in terms of the diagnostic age groups that we defined above and we show them as a series of pie diagrams arranged along the length of the main stream and major tributaries in order to show how the population of zircon ages within the river changes from the source to the river mouth. These pie diagrams only show the age character of the main stream and the tributaries and we do not attempt to indicate their relative importance as sediment sources to the mainstream. Only the uppermost diagram at Tuotuohe (#1) shows a significant population younger than 65 Ma, reflecting the young age of the basement in the Qamdo Block and the fact that the sediment eroded from this area is rapidly diluted by influx from the other rivers going downstream. As a general rule the overall character of the sediment is relatively continuous through the central part of the Yangtze Valley, although we note that the proportion of grains dating at 600–1000 Ma increases substantially downstream of Yibin (#9) (reaching 52%). This is perhaps not surprising because at this point the river and the local tributaries are flowing across the western part of the Yangtze Craton, whose bedrock contains a large proportion of zircons of this age (Fig. 2A). Further downstream we see an increase in the proportion of 100–300 Ma grains in the region of the Three Gorges, and this part of the population also increases in the region downstream of Hukou (#22).

Such significant changes in the age composition of the main stream downstream of a confluence suggests large-scale influx from the related tributaries into the main stream, thus changing the bulk composition. Because the total load tends to increase downstream we recognize that less sediment is required to change the net composition in the upper reaches compared to the lower reaches. We note that at Yueyang (#18) the proportion of 300–600 Ma grains is higher than further upstream (#15), although this proportion decreases somewhat downstream of this point because of further dilution from sediment supplied by tributaries joining the river at and downstream of Wuhan (#20). The oldest age group that we consider (2000–2700 Ma) reaches a minimum in the river around Yibin (#9), but then increases sharply again downstream at Chongqing (#11). This development indicates that some of the tributaries are providing large amounts of zircon to the main stream and are affecting the bulk composition. We note that this significant change is not limited to the upper reaches of the river, but indicates that tributaries joining the middle and lower reaches may also be providing large volumes of sediment, despite the fact that these tributaries are not draining the highest topography within the river basin.

Consideration of the zircon age populations in the tributaries can help us to understand why detrital records in the main stream evolve in the way they do. Fig. 5 highlights the significant differences between the different catchments as a result of the different bedrock lithologies and tectonic blocks, as well as erosion patterns within each of the tributary basins. As noted above, none of the tributaries contain unique single grain ages, but they differ from each other in the relative proportion of the different age groups that we have identified. For example, the Yalongjiang (#4) is noteworthy for being abundant in 600–1000 Ma grains, although we recognize that the Hanjiang (#19) and the Yuanjiang (#16) are also relatively rich in this particular population group (Fig. 5). In contrast, the Wujiang (#12) and Jialingjiang (#10) have high proportions of the 1700–2000 Ma zircons. The single sample that represents flux from the Daduhe (#6) and the Minjiang (#7,8) is characterized by particularly high abundances of 100–300 Ma zircons. 300–600 Ma zircons are especially abundant in the Xiangjiang (#17) and Ganjiang (#21). As a result of these distinctive signatures we would expect the river main stream composition to change sharply downstream of these confluences if the rivers are contributing large amounts of sediment to the Yangtze.

6.3. Downstream mixing

The downstream evolution of the detrital zircon populations in the Yangtze can be traced by plotting the proportion of each of the four

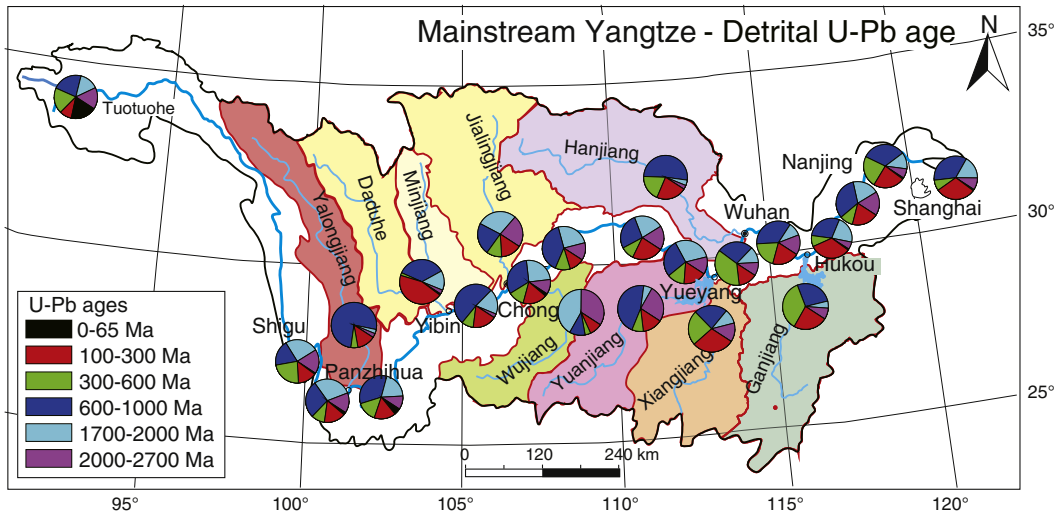

Fig. 5. Pie charts showing the range of zircon U–Pb ages for sands in the modern Yangtze main stream and major tributaries.

most abundant age groups for the main river and comparing those with the concentrations in the tributaries. Fig. 6 shows how the river evolves downstream in terms of the relative abundance of each age group. A continuous line shows the changing proportion of each age population within the main stream. Vertical lines show where the major tributaries join the main stream, with individual symbols showing the relative concentration in each tributary. When the composition of the tributaries is significantly different from the main river we would expect the bulk composition of the river to change significantly downstream of that confluence when the flux from the tributary is large and assuming similar concentrations of zircon in both main stream and tributaries (Amidon et al., 2005). However, when the tributaries have compositions close to the main stream then no change would be expected even if the flux from that river was significant. Because the total load is expected to increase downstream as more rivers join the flux greater volumes of sediment are required to change the net flow by a given percentage in the lower reaches compared to the upper reaches. Nonetheless, we note that the lower reaches and Sichuan Basin may be areas of sediment trapping and sequester, so that it is not a given that the total load must increase downstream and without sediment gauging data no ready correction can be made to determine total sediment flux from each tributary as a proportion of the flux to the ocean.

Correcting for relative zircon abundance in the main stream and tributaries is complicated but has been attempted in some studies

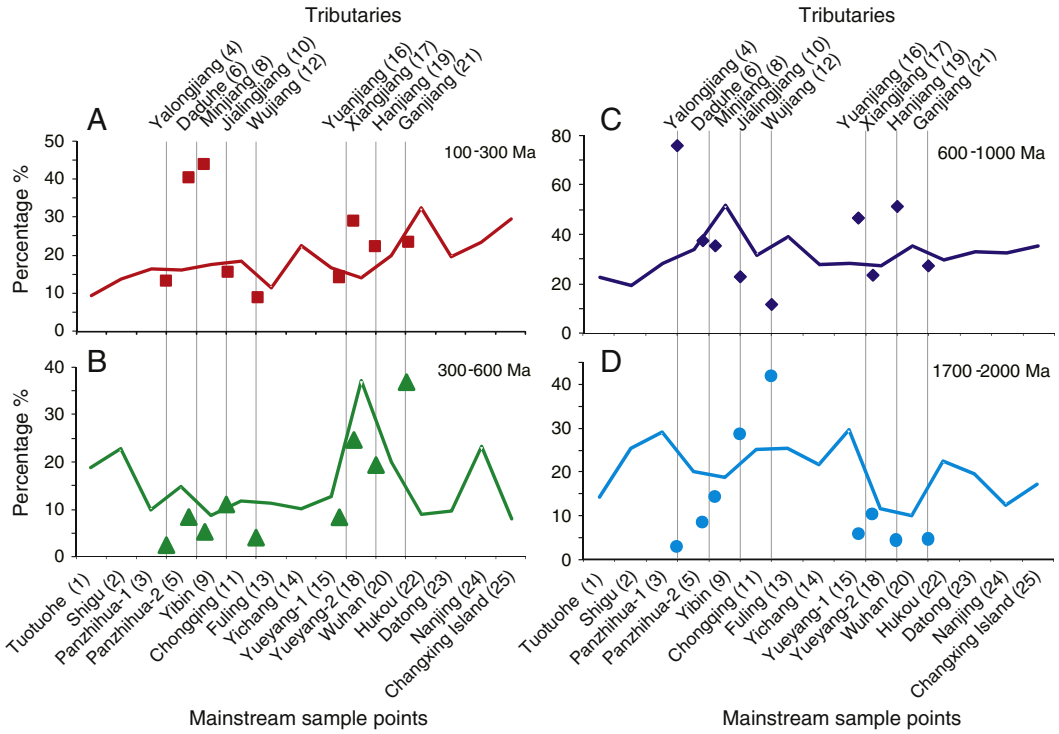

Fig. 6. Downstream evolution of zircon age populations in the Yangtze main stream. (A) 100–300 Ma (Indosinian), (B) 300–600 Ma (Caledonian-aged), (C) 600–1000 Ma (Yangtze Craton) and (D) 1700–2000 Ma (Lüliangian).

based on the Zr concentration in sand acting as a proxy for zircon abundance (Amidon et al., 2005), assuming that the sample is representative of the average flux in any given river. However, this correction may not be very accurate depending on exactly where in the stream the sample was taken. Current sorting may preferentially concentrate or dilute zircon in any particular sample relative to the average flux depending on where and when the sample is taken from the river channel. While sorting is unlikely to change the ages of the zircons sampled it can result in significant variations in relative concentration over short time and length scales. Unless we know that the river sand is representative of the total flux then making any type of correction will introduce additional uncertainties. In view of the large size of our drainage basins and therefore the unlikelihood that the source rocks are significantly different in total zircon concentration because of the diversity of source rocks within each sub-basin, we do not to try to correct for concentration because it is likely to add more uncertainty than it would resolve.

Fig. 6A shows the development in 100–300 Ma zircons. We note that the proportion of these grains in the Daduhe (#6) and Minjiang (#7,8) is very high, but that the river itself does not change downstream of that confluence, indicating that these are volumetric unimportant sources for detrital zircons. However, the proportion of this population decreases after the Yangtze joins the Wujiang (#12), indicating that this river is an important supplier of zircon. Interestingly, the proportion of this age group also increases sharply between the Wujiang (#12) and Yuanjiang (#16) confluences, which implies significant erosion along the main stream, and/or the contribution of small rivers. The Xiangjiang (#17) is relatively rich in the 100–300 Ma age population, but does not make an impression on the bulk composition in the Yangtze, despite the fact that heavy mineral analysis of this river indicated a high proportion of zircon in the sediment (Yang et al., 2009). In contrast, the Hanjiang (#19) is effective in increasing the proportion of this age group in the main river. In contrast, the Yangtze increases in the proportion of this age population downstream of the Ganjiang (#21) confluence, despite the low proportion in that river demonstrating that this is not a major sediment supplier.

We examine the relative influence of each tributary further by considering the 300–600 Ma population. Fig. 6B confirms that the Hanjiang (#19) is an important contributor of this age group and that the Ganjiang (#21) and the Yalongjiang (#4) are not significant. This population does allow for some influence from the Daduhe (#6)/Minjiang (#7,8) because these rivers are low in 300–600 Ma grains and the Yangtze shows decreasing abundance in this group downstream of the confluence. In contrast to the younger (100–300 Ma) age group, the 300–600 Ma population indicates that the Xiangjiang (#17) does appear to play an important role, whereas the Wujiang (#12) has little influence. The apparent bulk sediment contribution from the Xiangjiang (#17) may be less than we infer from the mixing diagram because this river may be especially rich in zircons (Yang et al., 2009). We also observe significant change in the river downstream of the Ganjiang (#21) confluence requiring sediment to be added to the mainstream downstream of Hukou. Because there is no major tributary joining the main stream in these lowermost reaches we suggest that this change in composition indicates local reworking, likely from Quaternary river flood plain deposits. These may be reworked during floods when the river's sediment carrying capacity is increased and entrenchment occurs. Holocene incision of river valleys into flood plains has been documented in the Sutlej (Bookhagen et al., 2006) and Indus River after 10 ka (Giosan et al., 2012). Capture of sediment behind the Three Gorges Dam has the potential to increase erosion of the flood plain downstream of Yichang, including those parts downstream of Hukou, but would also affect flood plains between Hukou and Yichang.

Consideration of the 600–1000 Ma population (Fig. 6C) provides further confidence that the Hanjiang (#19) is the most important zircon supplier and also indicates an important role for the Jialingjiang (#10), which we had been unable to assess using the younger age populations because of their similarity to the average composition in the Yangtze main stream. The 600–1000 Ma population reinforces the conclusion concerning the relative unimportance of the Daduhe (#6) and the Minjiang (#7,8), however the increase in 600–1000 Ma grains between Panzhihua-2 (#5) and Yibin (#9) requires significant addition of sediment, which we infer must be derived from along the main stream and/or from small rivers joining the Yangtze in this section. This age population also indicates relatively little addition from the Yalongjiang (#4) and the Wujiang (#12), and provides the opportunity for our first test of the Yuanjiang (#16), which despite being rich in this age group appears to exert little influence on the bulk composition of the main stream.

Finally, we examine the influence of the 1700–2000 Ma population (Fig. 6D). As with the other groups the Hanjiang (#19) shows a large change downstream of its confluence, while the Ganjiang (#21) seems to have negligible effect. The same is true of the Wujiang (#12). This 1700–2000 Ma age population argues for some influence from the Yalongjiang (#4), which had not been apparent in the other groups. Concentration of 1700–2000 Ma zircons in the main stream falls sharply downstream of the confluence with the Yuanjiang (#16) and the Xiangjiang (#17), and we favor the Xiangjiang (#17) as being the cause of this fall because the other population groups eliminate the probability that the Yuanjiang (#16) is the dominant supplier of sediment. This influence is consistent with the observation that the Xiangjiang (#17) is especially rich in zircon grains relative to other tributaries (Yang et al., 2009).

Calculating the percentage contributed by each tributary downstream of its confluence is possible if we treat each population group separately and assume the same concentrations of zircon in each stream, as we have for the other calculations (Table 3). In several cases an unrealistic answer is derived. For example, between Panzhihua-1 and Panzhihua-2 the river mixes with the Yalongjiang. If we consider the 300–600 Ma zircon populations then the concentration of these rises from 9% to 13% downstream of the confluence. However, the Yalongjiang contains only 5% of 300–600 Ma zircons, which would be expected to decrease the total after mixing. This result suggests that some of the samples were not representative of the net flow. It also implies that the Yalongjiang has little effect on the bulk flow compared to local sources. In other examples no meaningful number can be extracted because the samples have similar concentrations so that the uncertainties are very high. Greatest confidence can be expressed when the results from more than one population group are in accord, especially when those groups are abundant. Results that show disagreement between groups are usually the result of low zircon concentrations and thus high uncertainties, such as the prediction of 75% input from the Wujiang according to the 100–300 Ma zircons, but zero input from both the 600–1000 and 1700–2000 Ma groups (Table 3). In this case, the low proportion of 100–300 Ma zircons means that this number is unreliable. Nonetheless, some patterns do emerge, confirming that the Xiangjiang and Hanjiang are important net contributors to the total flux, but because of the scatter it is not possible to assign a single percentage for each tributary. We further recognize that because the total sediment load is expected to increase downstream

Table 3
Calculation net contribution of each tributary to the net flow in the main stream downstream of each confluence, estimated for each population group. NA = Not applicable, no meaningful result.

	100–300 Ma	300–600 Ma	600–1000 Ma	1700–2000 Ma
Yalongjiang	NA*	Low*	7	20
Dadu/Minjiang	7	NA	NA	Low
Jialingjiang	Low	100*	72	60
Wujiang	75	0	NA	0
Xiangjiang	30	High	NA*	70
Hanjiang	45	High	23	0*
Ganjiang	NA	Low	50*	Low

* = Low numbers or similar composition, i.e. high uncertainty.

as the river is joined by more tributaries that the total volume of sediment needed to make a difference to the bulk flow increases downstream. Thus, the estimate that 23–45% of the river load is derived from the Hanjiang downstream of its confluence with the mainstream is especially impressive, because it is one of the last tributaries to join the main stream.

Fig. 6 also allows us to conclude that the most important sediment contributor to the main Yangtze is the Hanjiang (#19), with significant flux also from the Xiangjiang (#17) and Jialingjiang (#10) and along the main stream between Panzhihua-2 (#5) and Yibin (#9). The least important rivers supplying sediment to the modern Yangtze River appear to be the Ganjiang (#21), the Daduhe (#6), the Minjiang (#7,8) and probably the Wujiang (#12). Other tributaries seem to have an intermediate effect on the composition of the bulk flow.

6.4. Factors impacting detrital zircon ages

We now consider the extent to which the sediments in the different tributaries are representative of the bedrock that is exposed within each of the river basins. In doing this we test the proposition by Amidon et al. (2005) and several other authors (Hodges et al., 2005; Huntington and Hodges, 2006) that rivers provide representative samples of the entire basin, across the width and height of the basin upstream of any sample point. Amidon et al. (2005) concluded this to be the case in the fluvially dynamic environment of the Nepalese Himalaya. To do this we compare the age population of the zircons in the river sediments with the anticipated age population that is based on the relative extent of exposure of different tectonic blocks within any given basin. The scale of the map we use is 1:12,500,000 (Pubellier et al., 2008) and is intended only to assess general patterns at the first order scale.

The basic geologic framework of central China, composed of different tectonic blocks is fairly well known and is unlikely to represent a large uncertainty. However, a greater source of uncertainty is the amount of U–Pb zircon dating available for the bedrocks and which we must presume to be uniform within each block because we lack detailed age dating across wide areas of bedrock within each tributary basin. Because we have some constraints on the age composition of each of the tectonic blocks (Fig. 2B) we can make a prediction about the age of zircons in sediment that would be formed if the basin was uniformly eroded and the source rocks equally rich in zircons. We do not expect this to be the case for every location, but we argue that this provides a baseline model against which we can compare our measured spectra. For example, following this argumentation, a basin which exposed 50% of the Songpan–Garze might be expected to have 50% of its zircons with the same average age spectrum as found in the basement samples from that terrain.

In predicting detrital grain ages we have to assume that the average measured from each tectonic block is representative of all of the outcrops assigned to that block from across the entire basin. Provided the percentage of the outcrops for a given block within any basin can be estimated then the contribution from that block to a uniform-erosion model can be calculated. Our predictions are provided in Table 4. Fig. 7 shows a comparison between the measured age populations and those anticipated in the event that erosion was uniform across each of the river basins. Our assessment of the "goodness of fit" between predicted and measured is done visually, because more quantitative assessments (e.g., the nonparametric Kolmogorov–Smirnov approach to test the equality of two distributions) do not take into account the uncertainties in the boundary conditions. The fit is considered to be good if the measured and predicted patterns have the same peaks in approximately the same proportion.

Fig. 7 shows that there is significant variability between the uniform-erosion model and measured sediments within the different tributaries. Nonetheless, three of the tributaries show very close comparison between the model and the measured, suggestive of relatively uniform erosion across these river basins, i.e., the Hanjiang (#19), the Minjiang (#7,8) and the Yuanjiang (#16). The Daduhe (#6) shows reasonably close correspondence; except for it having more 100–300 Ma grains and fewer 600–1000 Ma than might be anticipated. At the other extreme we see some basins where there is very little correspondence between the uniform-erosion model and the observed, and in particular we note that the Yalongjiang (#4) and Wujiang (#12), which appear to provide very poor representation of the average bedrock composition, thus implying focused erosion within those basins of specific rock types that dominate the bulk flux in the tributary. The other tributaries show some reasonable approximation, but with significant departures indicative of non-uniform erosion across their areas. In general many of the Yangtze tributaries seem to show evidence for significant localized erosion, although we recognize that the bedrock source may be more variable than has so far been documented, but this cannot be factored into our analysis and can only be improved by doing large amounts of additional bedrock dating. Future work on this topic may require a re-evaluation of this question. The generally large size of the Yangtze tributaries does at least favor the bedrock being close to the terrain-wide average and less affected by local heterogeneity.

In order to estimate the contributions of tributaries to the zircon load and main stream age distributions, we have calculated various weights for each catchment. In the most simple case with uniform climate and uniform topography (i.e., steepness, relief, elevation), the zircon

Table 4
Comparison of population percentage measured by U–Pb dating and uniform-erosion model predicted from the source bedrocks.

		Age (Ma) %					
		0–65	100–300	300–600	600–1000	1700–2000	2000–2700
Yalongjiang	Uniform-erosion model	0	22	27	19	20	13
	Measured	0	13	5	76	3	3
Daduhe	Uniform-erosion model	0	22	25	21	20	13
	Measured	0	40	9	37	9	5
Minjiang-2	Uniform-erosion model	0	21	12	37	19	11
	Measured	1	44	2	35	14	3
Jialingjiang	Uniform-erosion model	0	15	20	39	12	14
	Measured	0	15	11	23	29	23
Wujiang	Uniform-erosion model	0	20	0	52	18	10
	Measured	0	9	4	11	42	34
Yuanjiang	Uniform-erosion model	0	4	4	49	17	26
	Measured	0	14	8	46	6	25
Xiangjiang	Uniform-erosion model	0	8	7	41	20	25
	Measured	0	29	24	23	10	13
Hanjiang	Uniform-erosion model	0	23	29	35	7	8
	Measured	0	22	19	51	4	3
Ganjiang	Uniform-erosion model	0	8	7	41	20	25
	Measured	0	24	36	27	5	8

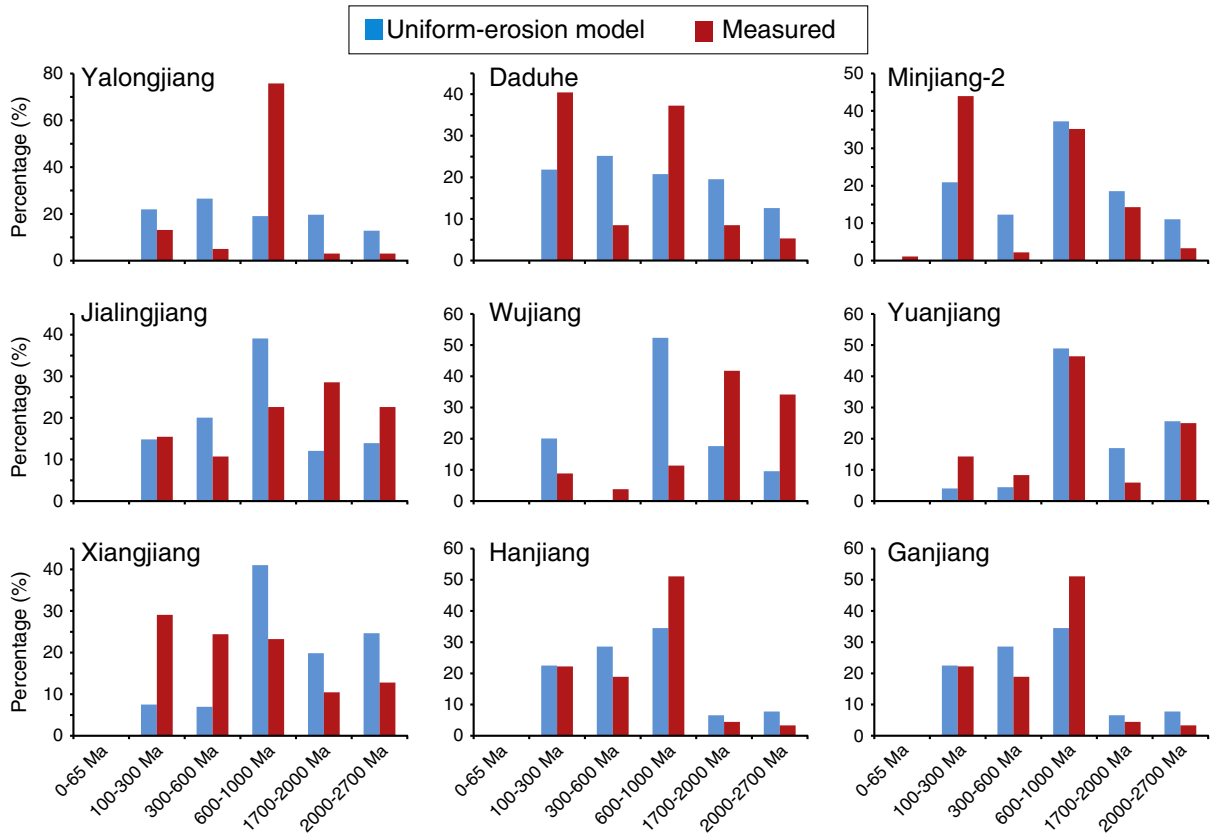

Fig. 7. Bar charts showing comparison of zircon populations within individual Yangtze River tributaries comparing the population measured by U–Pb dating and those predicted from the area of the outcrop and the previously established zircon age character of the source bedrock.

contribution should scale with drainage area. If the erosion were uniform in each basin then the size of the tributary basin would determine the relative influence of each stream to the overall discharge. We have derived the percentage contribution of each tributary by dividing the tributary areas by the catchment area of the entire Yangtze (i.e., at the outlet of the Yangtze into the East China Sea, the contribution is 100%). The areal contributions of the catchments vary generally between <5 and 13% (Fig. 8A). This prediction does not match the inferred provenance of the sand based on our analysis. Although the Jialingjiang (#10) and Hanjiang (#19) are predicted to be important sources and do provide large amount of zircon-bearing sediment we note that the main stream, upstream of Shigu (#2) would be the largest single provider, which we know is not the case.

Having identified those rivers that are producing the bulk of the sediment load to the main stream we now go on to consider what processes may be controlling the relative efficiency of sediment supply in each of the tributary basins because we know that it is not only dependent on basin area. Why do some tributaries provide a lot of sediment while others have little influence despite having significant drainage area? In order to answer this question, we analyze the relative discharge, channel steepness, and specific stream power contributions from each catchment. We assume that discharge is a reliable proxy for climate-driven erosion that channel steepness is largely an indicator of tectonically-controlled rock uplift, and that specific stream power is a combination of both, because it depends on discharge and channel steepness.

6.4.1. Impact of climate

Precipitation might be expected to be an important control on erosion because it is the primary control on discharge. In Fig. 1B we show the annual average precipitation across the basin as measured by Tropical Rainfall Measuring Mission (TRMM) satellite measurements (see Bookhagen and Burbank (2010) for processing details). There is a clear gradient from West to East going from relatively dry conditions in the upstream parts in Tibet to relatively heavy precipitation in the East, and especially in the southeast, most particularly the Ganjiang (#21) and Xiangjiang (#17) basins. While the latter appears to have some importance in supplying sediment the relative inefficiency of the Ganjiang (#21) it is in stark contrast to the fact that this is the wettest tributary basin. The highly sediment productive tributaries in the central part of the Yangtze basin, the Hanjiang (#19) and Jialingjiang (#10), as well as the lower Jinshajiang between Panzhihua-2 (#5) and Yibin (#9) receive an intermediate amount of rainfall and show no obvious difference in precipitation compared to the relatively unproductive basins of the Wujiang (#12) and Yuanjiang (#16).

We attempt to see if discharge is a controlling factor for zircon load in the streams. Higher discharges are expected to result in higher zircon loads, assuming that the bedrock sources are actually zircon bearing. Discharge contributions were calculated from the TRMM 2B31 rainfall data and are shown in Fig. 8B (Bookhagen and Burbank, 2010). These discharges agree well with discharge-gauge measurements at various sites along the Yangtze River (Fig. S2). We show the percentage discharge contribution for each catchment (outlet of the Yangtze is 100%) in Fig. 8B. The catchment contributions vary between <5 and 12%, with the lowest values in the driest catchments. Note the differences between areal (no precipitation gradient) and discharge (based on precipitation data) contribution. We consider discharge (or any other potential influence) to be influential in controlling erosion if there is a correlation between this factor and the tributary basins that are most important in changing the bulk character of the Yangtze (i.e., that add a lot of sediment to the river at the confluence). Some judgment is required to determine whether the fit is good or not.

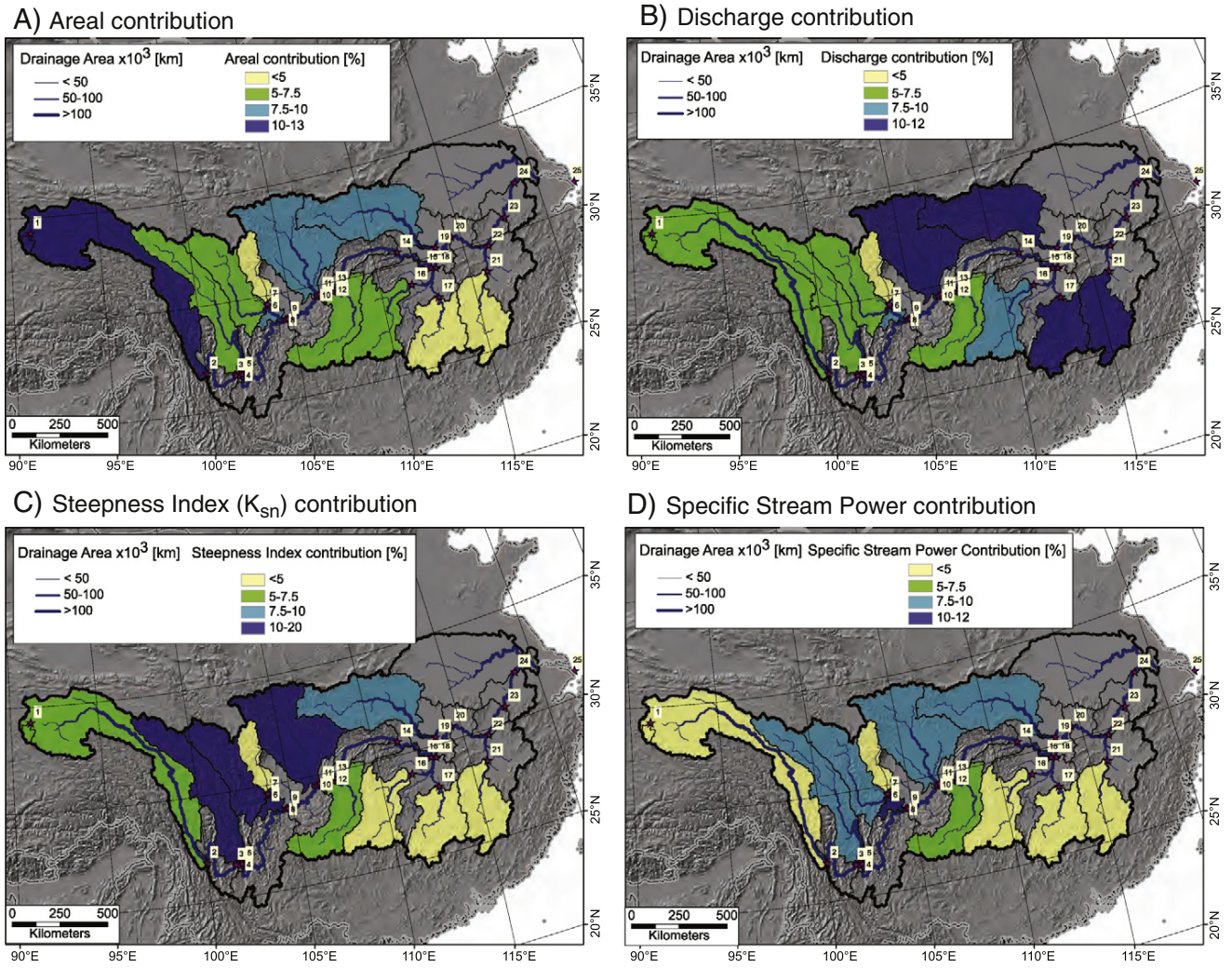

Fig. 8. Maps showing the predicted contribution of each of the Yangtze tributaries to the net sediment flux based on (A) the area of the tributary basin, (B) the discharge of water from each tributary, (C) the steepness of river channels within each basin and (D) the calculated specific stream power for each tributary.

While our discharge model successfully predicts the important flux from the Jialingjiang (#10) and the Hanjiang (#19), as well as low flux from the Jinshajiang, it fails to predict the low zircon flux from the Xiangjiang (#17) and Ganjiang (#21). We conclude that precipitation is not the dominant influence on sediment production in the modern river system.

However, we need to consider how past climate may have affected the Yangtze erosion patterns. Although suspended sediments can be transported quickly from source to sink the zircon grains we consider here are not generally transported in this fashion but instead as bedload, which moves more slowly through the system. Available U-series dating of sediment in the Ganges River for example suggests long transport times of ca. 100 k.y. for sediments traveling between the range front and the delta (ca. 1650 km) (Chabaux et al., 2006; Granet et al., 2007), although residence times were estimated to be shorter (~25 k.y.) for finer grained sediment (Granet et al., 2010). Most recently ^{10}Be cosmogenic dating argues for sediment transfer times of ~1400 years in the Ganges (Lupker et al., 2012) consistent with the similar short residence times deduced in the Andean foreland (Wittmann et al., 2011). Clift and Giosan (2013) estimate a transport time of 5000–10,000 years for zircon grains in the Indus River, which suggests a similar order of magnitude for zircon travel times in the Yangtze, similar to the thousands of years transport time inferred from Red River zircons (Hoang et al., 2010).

In this case we should consider how rainfall patterns may have influenced erosion during the Early Holocene. Speleothem records from caves in eastern and central China provide evidence for a stronger summer monsoon in the Early Holocene compared to the present day (Wang et al., 2001; Dykoski et al., 2005; Yang et al., 2010). This would have resulted in a westward advance of the summer monsoon rain front into the valleys of the eastern Tibetan Plateau, and also in the intensification of summer rain in the middle reaches of the river. Because the rainfall is presently already very strong in the eastern coastal parts of the basin (Fig. 1B) we would not anticipate a major increase in rainfall in that area during the Early Holocene. Although we do not see significant erosion from the tributaries in the upper reaches that might be linked to a stronger Early Holocene monsoon it is possible that the high sediment production in the middle part of the basin could be linked to heavier rainfall relative to the eastern lower reaches at that time. This erosion would only now be affecting the bulk composition of the Yangtze main stream.

6.4.2. Impact of tectonic forcing

In order to understand the influence of tectonic activity in controlling erosion efficiency we use the location of earthquake data to identify those regions that are currently experiencing active deformation, generally compressional and driving rock uplift in eastern Tibet and SW

China. It has been argued that tectonically driven rock uplift will steepen slopes and is an important control on erosion rates (Burbank and Anderson, 2001; Burbank et al., 2003). Seismic shaking also enhances mass wasting and sediment transport. However, the region around an epicenter where erosion is enhanced is not easily defined because it depends on several variables, not least the size and depth of the earthquake. In making this comparison we only aim to show where deformation and earthquake shaking are active and if there is a first order correlation with sediment yield in the different tributary basins, not on a smaller scale. We recognize that as well as the simple distribution and magnitude of earthquakes we consider here that peak ground acceleration combined with threshold slopes is really required to understand the ability of seismicity to drive sediment transport. Such a treatment lies outside the scope of this work, which in any case integrates sediment production and transport over thousands of years not just the short time over which detailed seismic data are available. Fig. 1A shows the location of earthquakes of magnitude 5 and greater dating back to 1973 as derived from US Geological Survey and National Earthquake Information Center (Ryan et al., 2009). This map shows stronger tectonic deformation in the western part of the Yangtze basin and especially affecting the Yalongjiang (#4), Daduhe (#6), Minjiang (#7,8) and to a lesser extent the Jialingjiang (#10). It is immediately clear that the pattern of present-day seismic shaking cannot be the primary control on sediment production, although the main stream between Panzhihua-2 (#5) and Yibin (#9) is both sediment productive and seismically active. Of the seismically active major tributary basins only the Jialingjiang (#10) appears to have a strong influence on the bulk composition of the Yangtze main stream, and while there is abundant evidence of erosion in other river systems they do not apparently strongly affect the total composition in the main stream.

We now consider the effect of topographic steepness on erosion efficiency because high rainfall in the absence of slope is unlikely to result in rapid erosion and sediment production (Kirby and Whipple, 2012). Steepness indices essentially integrate seismic evolution over geologic timescales, i.e., high seismic activity and rock deformation lead to steeper terrain over several earthquake cycles and hence to higher steepness indices. Higher steepness indices have been argued to relate to higher erosion rates and/or exhumation rates (Ouimet et al., 2009; Cyr et al., 2010). We recognize the fact that total altitude is not especially important, but that the steepness of the channel slopes can be a determining factor because high slope gradients are more liable to rapid soil motion and to landsliding. Fig. 9 shows the spatial variation in steepness indices (k_{sn}) as calculated from channel slopes using Shuttle Radar Topography Mission (SRTM) data (Wobus et al., 2006). We use the normalized steepness index (k_{sn}), which corrects for the influence of basin area and channel concavity, using a reference concavity for all the areas being considered. This approach calculates the normalized steepness when a regression with the fixed reference concavity (0.45) is forced through channel slope versus drainage area to yield the best fit. Magnitudes of steepness indices have been previously linked to erosional magnitude in parts of the study area (Ouimet et al., 2009). This map was created by calculating the steepness indices for all channels from the 90-m SRTM DEM with drainage areas >1 km^2 and then applying a 5-km smoothing window interpolation to form a spatially coherent map view (see Bookhagen and Strecker (2012) for details). We note that all quantitative data were derived from the uninterpolated data. We prefer channel steepness instead of hillslope angles as a proxy for landscape erosion, because hillslope angles attain their threshold values rather quickly, but channel steepness values continue to increase, even when hillslope angles have reached their threshold angle (e.g., Ouimet

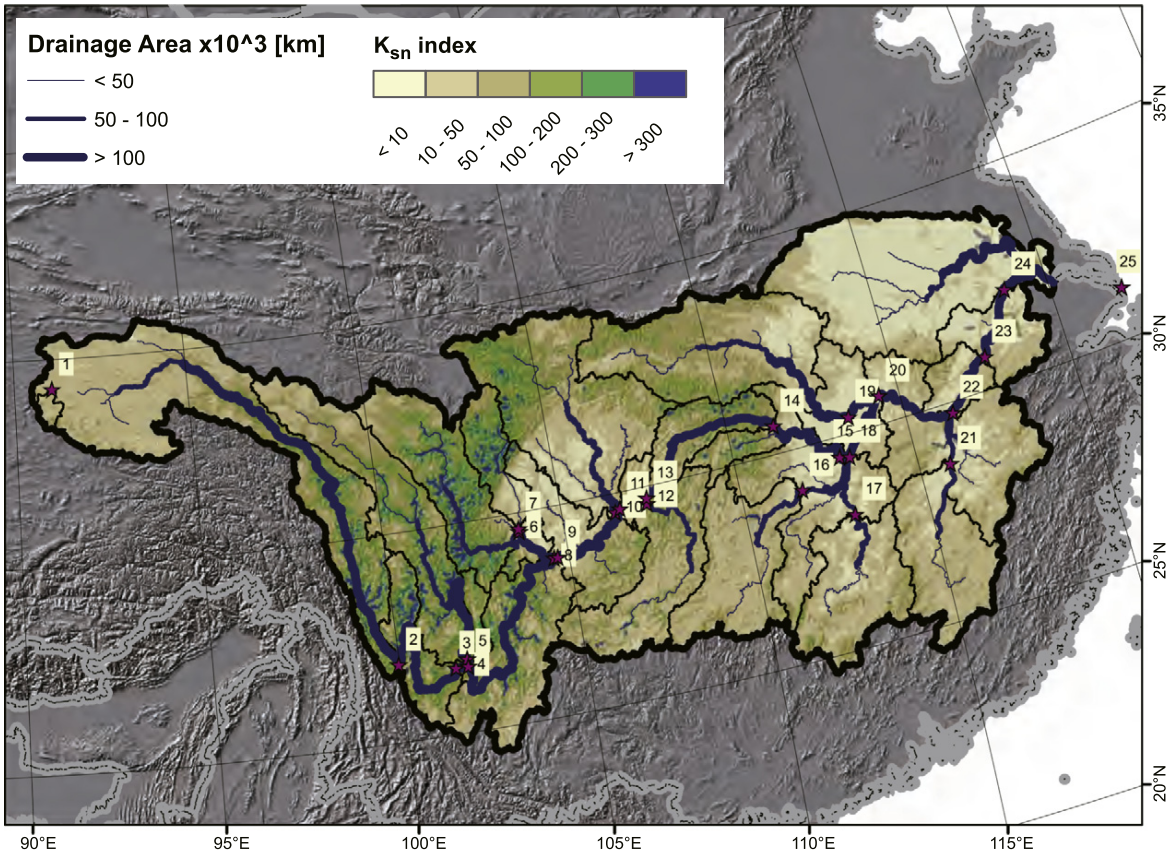

Fig. 9. Map showing spatial variations in steepness of the Yangtze Basin as measured from the steepness index (K_{sn}). The steepness index has been calculated for all catchment with drainage area >1 km^2 and this map view includes a 5-km smoothing window interpolation for viewing purposes.

et al., 2009). The map identifies the steepest regions as lying in the Jinshajiang upstream of the First Bend, as well as within the Yalongjiang (#4), Daduhe (#6) and Minjiang (#7,8). As described above, these parts of the drainage system do not appear to be dominant contributors to the modern river and so we infer that steepness of slope is not the primary cause of sediment production in the modern river.

We now use the steepness-index spatial pattern to calculate the percentage contribution of each tributary using the ratio of the sum of all steepness values for each catchment vs. the entire Yangtze catchment (Fig. 8C). Generally low-slope, lower-elevation catchments have very low net sediment contributions (<5%). This is in stark contrast to the discharge contribution. Note the very high, predicted contributions of some of the steeper catchments on the border of the eastern Tibetan Plateau (up to 20%). The model predicts high contributions from the Yalongjiang (#4) and the Daduhe (#6), whereas our budget indicated that these were not volumetrically important. We therefore conclude, based on both the earthquake and steepness data, that present-day tectonic processes are not currently the dominant control on detrital zircon erosion in the Yangtze basin, except along the lower parts of the Jinshajiang, although we do not exclude a tectonic influence over longer periods of geological time, as deep exhumation often requires this.

In order to combine climatic influences and terrain steepness, we have calculated specific stream power values for all pixels with drainage areas > 10 km^2 (Fig. 8D). Dry and low-slope catchments have low overall contributions (i.e., catchments originating from the Tibetan Plateau and tributaries in the low-elevation downstream section of the Yangtze). This model provides the best approximation of any of those we consider for predicting which tributaries are providing the most zircons to the main stream. The model is successful in indicating the importance of the Hanjiang (#19) and Jiangjiang, but overpredicts the influence of the Yalongjiang (#4) and the Daduhe (#6). Thus stream power, which largely reflects the combined influence of tectonics in causing steep slopes and climate, which controls precipitation and thus discharge, does appear to explain much of the variation in the modern river, but still cannot account for the entire zircon budget.

6.4.3. Impact of bedrock composition

We now examine the effect of lithologic composition on the ability of a tributary to provide sediment to the main stream. Fig. 10A shows

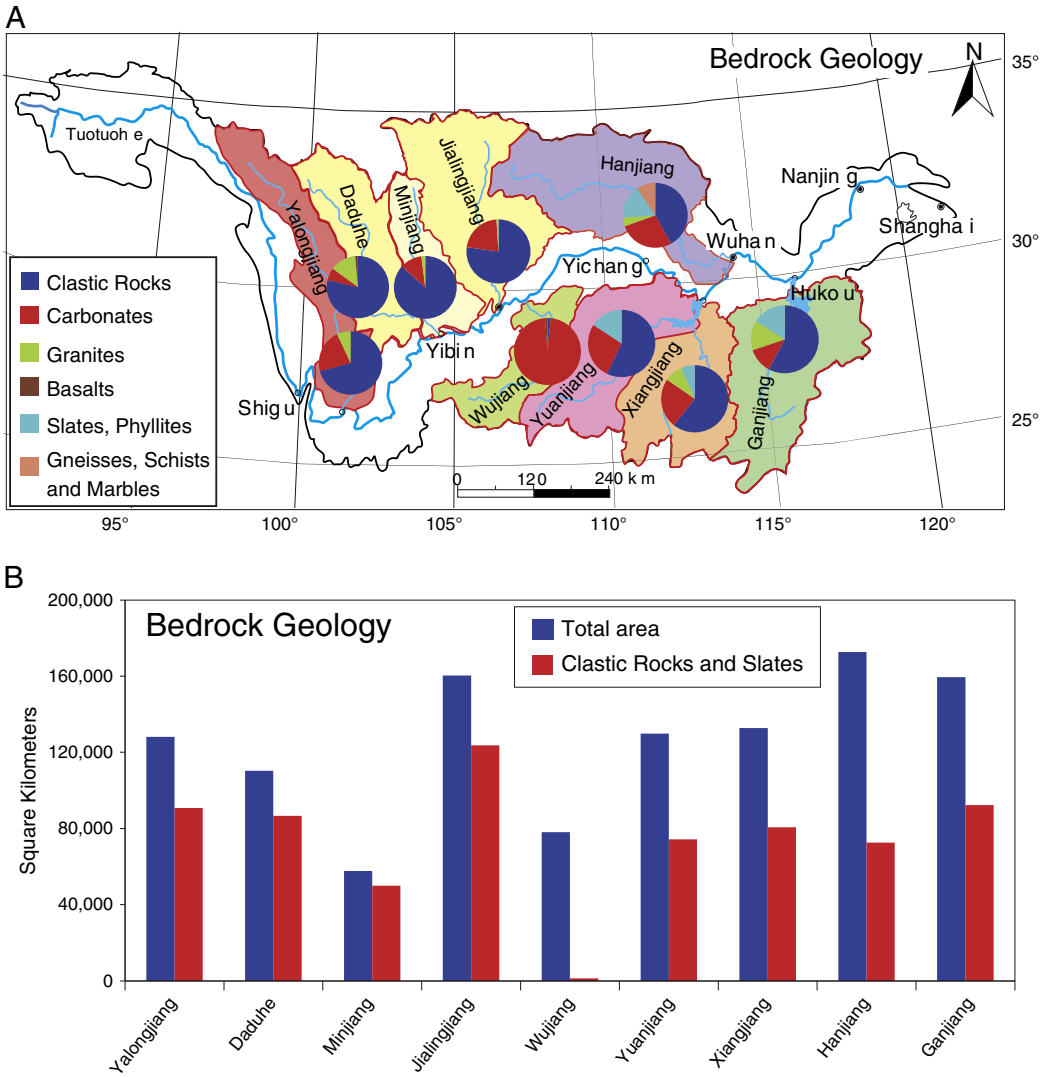

Fig. 10. (A) Diagram showing the overall lithological variations between the major tributaries of the Yangtze River in order to demonstrate large-scale changes in bedrock type that could affect the ability of the basin to act as a source of zircons to the modern river. (B) Bar chart showing the total basin area and the area occupied by readily eroded, zircon-bearing sedimentary and low-grade metamorphic rock types within each of the major tributary basins of the Yangtze River. Note that the Jialingjiang has the largest exposure of such rock types but that the Hanjiang is not unusual compared to other eastern tributaries in being a possible source of erodible bedrock.

the average variety of different rock types that comprise the outcrop in each of the major tributary basins. The Wujiang (#12) stands out in being the only basin that is almost completely dominated by carbonates. This clearly explains why this river does not supply many zircon grains to the main stream. However, lithologic variation is not a clear control in other parts of the Yangtze. The Hanjiang (#19) basin comprises approximately 25% carbonate, yet this tributary is the most zircon productive of any. It is the only basin with a substantial proportion of gneisses, which could be zircon-rich, although these are still strongly in the minority of the total and are generally considered rather hard and difficult to erode. We note the relative similarity of the outcrop between the productive Xiangjiang (#17) and sediment-poor Ganjiang (#21), suggesting that lithology is not a first-order control on the ability of the tributary to supply zircons to the main stream, provided the basin is not carbonate-dominated. We do not think that Holocene climate change can account for the differences between the Xiangjiang and the Ganjiang, because there is no reason to think that two adjacent low-land tributaries would be anti-correlated. We have no evidence that the Ganjiang is or was a major sediment producer. Likewise, in the northern parts of the basin we see similar bedrock lithologies in the Daduhe (#6), Minjiang (#7,8) and Jialingjiang (#10), and note that it is only the last of these rivers, which contributes significant amounts of sediment into the main stream.

Fig. 10B shows the total outcrop areas of the basins and compares them with the total area that is underlain by clastic sedimentary rocks and slates, which might be considered good sources of zircon and which might be more erodible than hard rocks, such as granites or gneisses. We note that the Jialingjiang (#10) has the largest single extent of these clastic sedimentary rocks and is also a strong producer of sediment to the main stream. However, the Hanjiang (#19) has less outcrop area of clastic sedimentary rocks compared to many and is not much different from the Ganjiang (#21) or Daduhe (#6), although it is much more sediment productive. We conclude that lithology, and particularly the presence of zircon-bearing clastic sedimentary rocks, is not a primary control in providing zircon to the modern Yangtze main stream, except in the case when there is almost no clastic rock exposed at all, in which case the contribution must tend to zero, as in the Wujiang (#12).

6.4.4. Impact of land degradation through human disturbances

We now consider the effect of human disturbance on the drainage basin as a mechanism for driving erosion. It has been recognized that human activities, especially widespread agriculture can result in accelerated erosion because plowing of the landscape allows more ready reworking of soils into the river systems, so that settlement is often followed by a pulse of sediment delivery into rivers and subsequently to the coast (Montgomery, 2007; Syvitski and Kettner, 2011). For example, the settlement of the Congo River Valley has been shown to result in a pulse of sediment delivery to the river mouth as a result of the start of intensive agriculture (Bayon et al., 2012). Likewise, studies of the Pearl River in southern China show enhanced reworking of ancient soils ~2500 years ago, at a time when that region was undergoing initial dense settlement and establishment of farming (Hu et al., 2013). More recently the introduction of damming has had the opposite effect, where human activities have reduced the flux of sediment into the ocean (Syvitski et al., 2005). Because we do not see a close correlation between our sediment production and natural processes we investigate the possibility that human settlement of the Yangtze Valley is at least partly controlling the rate of sediment production. The modern valley is very densely settled and is dominated by agriculture in the eastern two thirds, where almost no land is left in a natural state (Fig. 11A). Only the upper reaches show extensive tracts of original grassland and forest. We particularly consider the impact of initial settlement of the valley because we are relying on zircon sand grains, which are anticipated to take thousands of years to travel the length of the Yangtze, as discussed above. If transport is spanning thousands of years or more then modern disturbances should be less important in controlling zircon sediment production. A recent study from the Indus estimated that zircons are traveling through that river at a rate of 0.3–0.6 km/yr during the Holocene (Clift and Giosan, 2013), although presumably faster in the topographically steep upper reaches than in the flood plains. Nonetheless, if these rates are at all comparable to the Yangtze then it implies only 15–30 km of transport since the start of the post-World War II industrial period and just 190–390 km since the start of the Ming Dynasty. By comparison the Hanjiang alone is 1532 km long so that modern agriculture or damming is unlikely to have influenced the zircons flux. As a result we do not expect that modern human activities have had a major impact on the zircon population at the basin-wide scale, although they certainly control the source of sediment for the less dense and fine-grained minerals now in the Yangtze River (He et al., 2013b).

Fig. 11B shows a map of archeological sites within the Yangtze basin and provides us with the opportunity to understand how human settlement has spread through the valley in the last 10,000 years. As might be expected the oldest settlements are restricted to the lower reaches and close to the Three Gorges. After 5000 BCE (7 ka) there was a much wider settlement that extended into the middle reaches, although we note that it is generally still downstream of the Sichuan Basin. In particular, we see a lack of archeological sites in the upper reaches of the river and we speculate that it is the absence of widespread agriculture during early human history that has caused the relative lack of sediment production in the Yalongjiang (#4), Daduhe (#6) and Minjiang (#7,8) Rivers, despite the fact that the topography in this area is steep, and despite the occurrence of major earthquakes and significant monsoon rainfall, especially in the eastern parts of these tributary basins adjacent to the Sichuan Basin. We note that the Hanjiang basin (#19) experienced widespread settlement after 5000 BCE and is the most sediment productive tributary that we studied. Early settlements around the Three Gorges, downstream of Yichang (#14), open up the possibility that this region was also producing significant zircon-bearing sediment directly into the main stream. These areas appear not only to be regions of early settlement, but more importantly they are also regions of steep topography and high stream power. Although a correlation does not prove that early agriculture is the cause of sedimentary zircon production, it is nonetheless significant given the otherwise poor correlation of potential natural controls and the evidence from other areas that humans can act as geological agents at the largest scales.

We note that the degree of early settlement in the Ganjiang (#21) is relatively moderate, as it is in the adjacent Xiangjiang (#17). These two rivers are quite different in their sediment production so that we cannot attribute all the variation to human settlement. Both of these rivers are affected by major lakes that separate the bulk of the drainage from the Yangtze main stream. It is possible that the lakes are regulating the flux of sediment from the upper parts of these tributaries, although it is presently unclear why one would be releasing sediment into the Xiangjiang, while the other is buffering sediment flux into the main stream.

We conclude that it is the combination of erosive stream power and human settlement, which encourages basins to release significant volumes of sediment to the main stream following the onset of agriculture. Agriculture is the key process we associate with enhanced erosion because of its disruption of the soil profile, which will liberate more sediment of a range of grain sizes into the river systems, in contrast with the less erosive impact of hunter-gatherer societies (Montgomery, 2007). Archeological evidence now suggests that the Neolithic was a time of accelerating agriculture across much of central China (Li et al., 2007; Weisskopf, 2010; Zhang et al., 2010). The lack of early settlement in the upper reaches correlates at the first order with the relative lack of zircon production in that region, despite other favorable conditions that might otherwise encourage rapid erosion under natural conditions. The correlation of early settlement and sediment production does not prove that this is the key control on erosion in the modern system, but it significant and provides a better potential fit than any other single process.

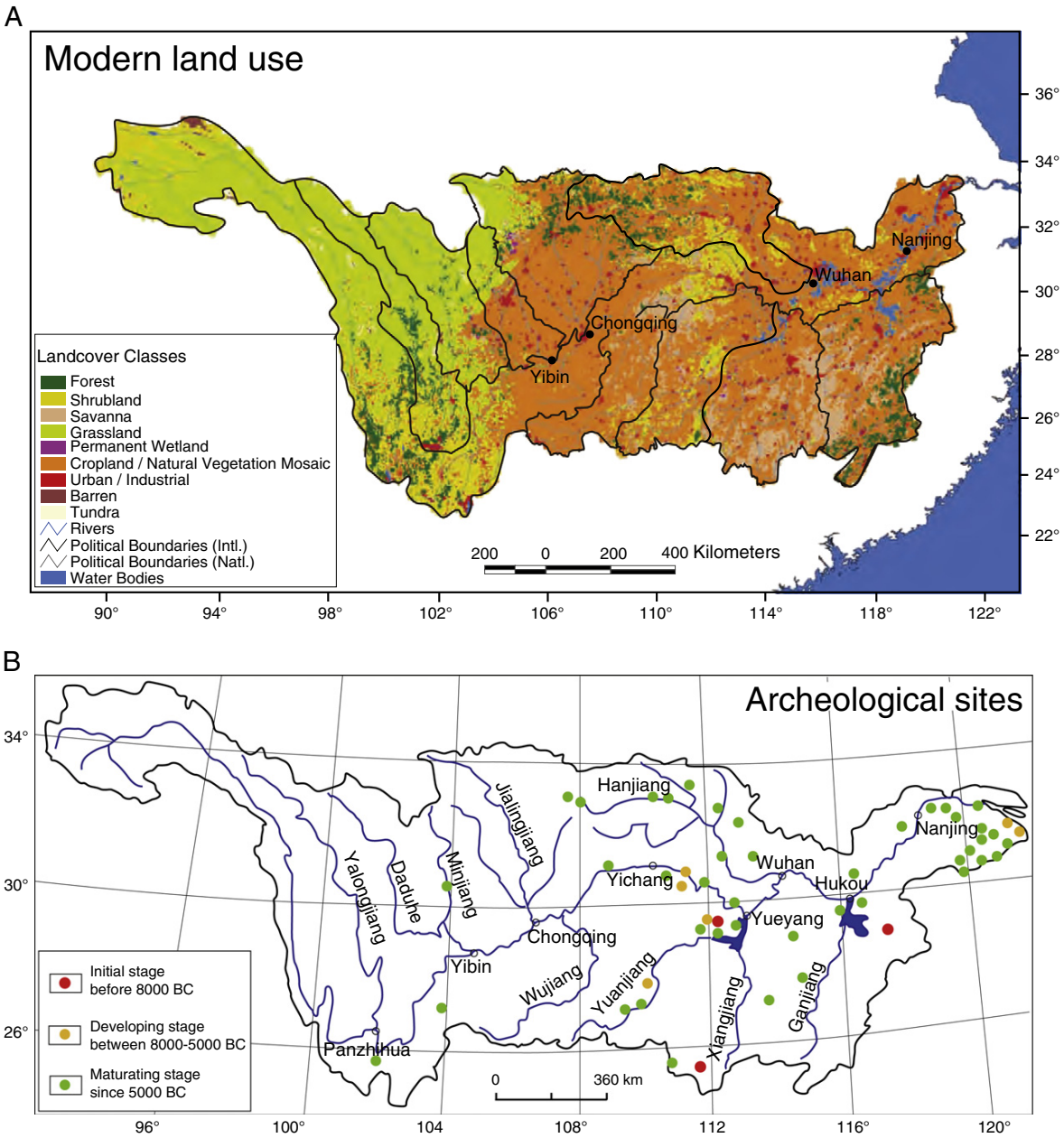

Fig. 11. (A) Map of land-use across the Yangtze Basin showing the modern dominance of farmland in the central and eastern parts of the drainage, while grassland dominates the upper reaches of the Yalongjiang and the Jinshajiang. Data from World Resources Institute (2003). (B) Map showing distribution of known archeology sites in the Yangtze basin at (A) >8 ka, (B) 8–5 ka and (C) <5 ka (Wu et al., 2012).

7. Conclusions

In this study we present for the first time a comprehensive survey of the U–Pb ages of zircon sand grains within the main stream of the Yangtze River and its major tributaries. We demonstrate that these have significant variation between the downstream and upstream regions and that this is largely related to ages in the basement source rocks. Comparison between the expected compositions based on bedrock ages and assuming uniform erosion and the zircon ages measured in the major tributaries demonstrates the fact that erosion cannot have been uniform across these basins except to a certain extent in the case of the Hanjiang (#19) and Yuanjiang (#16). Localized focused erosion is probably the result of topography, orographic rainfall and tectonically driven uplift within a single tributary basin. By splitting up the total zircon population into a number of key age groups we are able to assess which rivers are contributing large volumes of sediment into the main stream.

In particular, we identify the Hanjiang (#19), Xiangjiang (#17) and Jialingjiang (#10), as well as the Jinshajiang between Panzhihua-2 (#5) and Yibin (#9) as being the most important producers of zircon-rich sediment. The increasing sediment load downstream means that the influence of those rivers that join the river closer to the ocean is greater than those closer to the upstream area. This realization emphasizes the role of the Hanjiang (#19), and Xiangjiang (#17). We note that these tributaries occupy the middle reaches of the river and contrast with tectonically active, elevated areas in the upper reaches, which appear to contribute relatively moderate amounts of sediment to the total modern flow. Only the Jinshajiang between Panzhihua-2 (#5) and Yibin (#9) produces large volumes of sediment and is both tectonically active

and moderately wet in climate. Sediment production in the modern river does not correlate well with present-day earthquake activity or slope steepness, which we employ as first order proxies for active rock deformation on longer time scales.

We further see very little correlation between modern precipitation, discharge, and the contribution of zircon to the main stream. Climate reconstructions for the early part of the Holocene however would suggest stronger rainfall in the middle reaches at that time and the modern distribution of zircons in the river may reflect a pulse of erosion dating from that time because of the slow transport time for zircon grains through the river system. Although topographic steepness might be expected to be a primary control on sediment production and it is the western areas of the basin that have the steepest slopes, these do not appear to be the most sediment productive. However, the Jialingjiang (#10), Hanjiang (#19) and Jinshajiang between Panzhihua-2 (#5) and Yibin (#9) do produce a lot of sediment and are also regions of relatively steep slope and high specific stream power. Specific stream power is identified as the dominant natural control on sediment production.

We suggest that the most important single factor in controlling sediment production in the modern Yangtze is the disturbance of the landscape by human settlement in regions but only in areas where specific stream power is also high. In particular, we note that the middle reaches of the river were settled after around 5000 BCE and that these regions are now the most productive in terms of sediment yield. The eastern parts of the basin were also settled early in human history, but are not very sediment productive likely because of their relatively flat topography and low specific stream power. Thus, it is the combination of human settlement, steep topography and at least moderate amounts of rainfall that is most likely to have focused sediment production within the modern middle reaches of the Yangtze River basin.

We conclude that the present zircon load of the modern Yangtze River basin does not represent a natural system, but that important lessons concerning controls on erosion processes can nonetheless be learnt from consideration of the zircons in the modern river.

Supplementary data to this article can be found online at http://dx.doi.org/10.1016/j.earscirev.2014.05.014.

Acknowledgments

This study was supported by the “Strategic Priority Research Program” of the Chinese Academy of Sciences (grant no. XDB03020300), the China Geological Survey: Continental Shelf Drilling Program (project no. GZH201100202), the Natural Science Foundation of China (project no. 40930107 and 41111140016), and the United Nations Educational, Scientific and Cultural Organization (project no. IGCP–581). We thank the State Key Laboratory for Mineral Deposits Research, Nanjing University and Louisiana State University, the Charles T. McCord Chair, and all researchers who helped us with this article.

References

Amidon, W.H., Burbank, D.W., Gehrels, G.E., 2005. Construction of detrital mineral populations: insights from mixing of U–Pb zircon ages in Himalayan rivers. Basin Res. 17 (4), 463–485.

Andersen, T., 2002. Correction of common Pb in U–Pb analyses that do not report ^{204}Pb. Chem. Geol. 192, 59–79.

Bayon, G., Dennielou, B., Etoubleau, J., Ponzevera, E., Toucanne, S., Bermell, S., 2012. Intensifying weathering and land use in Iron Age Central Africa. Science 335 (6073), 1219–1222.

Berner, R.A., Berner, E.K., 1997. Silicate weathering and climate. In: Ruddiman, W.F. (Ed.), Tectonic Uplift and Climate Change. Springer, New York, pp. 353–365.

Black, L.P., Gulson, B.L., 1978. The age of the Mud Tank carbonatite, Strangways Range, Northern Territory. J. Aust. Geol. Geophys. 3, 227–232.

Bookhagen, B., Burbank, D.W., 2010. Towards a complete Himalayan hydrological budget: the spatiotemporal distribution of snow melt and rainfall and their impact on river discharge. J. Geophys. Res. 115, F03019.

Bookhagen, B., Strecker, M.R., 2012. Spatiotemporal trends in erosion rates across a pronounced rainfall gradient: examples from the southern Central Andes. Earth Planet. Sci. Lett. 327–328, 97–110.

Bookhagen, B., Fleitmann, D., Nishiizumi, K., Strecker, M.R., Thiede, R.C., 2006. Holocene Monsoonal dynamics and fluvial terrace formation in the northwest Himalaya, India. Geology 34 (7), 601–604.

Bruguier, O., Lancelot, J.R., Malavieille, J., 1997. U-Pb dating on single detrital zircon grains from the Triassic Songpan–Ganze flysch (Central China): provenance and tectonic correlations. Earth Planet. Sci. Lett. 152 (1–4), 217–231.

Burbank, D.W., Anderson, R.S., 2001. Tectonic Geomorphology. Blackwell, Oxford, p. 270.

Burbank, D.W., Blythe, A.E., Putkonen, J., Pratt-Sitaula, B., Gabet, E., Oskins, M., Barros, A., Ojha, T.P., 2003. Decoupling of erosion and precipitation in the Himalayas. Nature 426, 652–655.

Carter, A., Clift, P.D., 2008. Was the Indosinian orogeny a Triassic mountain building or thermotectonic reactivation event? C.R. Acad. Sci., Geosci. 340, 83–93.

Chabaux, F., Granet, M., Pelt, E., France-Lanord, C., Galy, V., 2006. U-238-U-234-Th-230 disequilibria and timescale of sedimentary transfers in rivers: clues from the Gangetic plain rivers. J. Geochem. Explor. 88, 373–375.

Chappell, J., Zheng, H., Fifield, K., 2006. Yangtse River sediments and erosion rates from source to sink traced with cosmogenic ^{10}Be: sediments from major rivers. Palaeogeogr. Palaeoclimatol. Palaeoecol. 241, 79–94.

Chen, S.F., Wilson, C.J.L., 1996. Emplacement of the Longmen Shan thrust-nappe belt along the eastern margin of the Tibetan Plateau. J. Struct. Geol. 18, 413–440.

Chen, Z.Y., Lu, L.Z., Gupta, A., 2001. The Yangtze River: an introduction. Geomorphology 41 (2–3), 73–75.

Chung, S.L., Jahn, B.M., 1995. Plume–lithosphere interaction in generation of the Emeishan flood basalts at the Permian–Triassic boundary. Geology 23, 889–892.

Clift, P.D., Giosan, L., 2013. Sediment fluxes and buffering in the post-glacial Indus Basin. Basin Res. 25, 1–18.

Compston, W., Williams, I.S., Kirschvink, J.L., Zhang, Z., Ma, G., 1992. Zircon U–Pb ages for the Early Cambrian time-scale. J. Geol. Soc. Lond. 149, 171–184.

Cyr, A.J., Granger, D.E., Olivetti, V., Molin, P., 2010. Quantifying rock uplift rates using channel steepness and cosmogenic nuclide-determined erosion rates: examples from northern and southern Italy. Lithosphere 2 (3), 188–198.

Ding, T., Wan, D., Wang, C., Zhang, F., 2004. Silicon isotope compositions of dissolved silicon and suspended matter in the Yangtze River, China. Geochim. Cosmochim. Acta 68 (2), 205–216.

Du, D.X., Luo, J.N., Li, X.Z., 1997. Sedimentary evolution and palaeogeography of the Qamdo Block in Xizang. Lithofacies Palaeogeogr. 17 (4), 1–17.

Dykoski, C.A., Edwards, R.L., Cheng, H., Yuan, D., Cai, Y., Zhang, M., Lin, Y., Qing, J., An, Z., Revenaugh, J., 2005. A high-resolution, absolute-dated Holocene and deglacial Asian monsoon record from Dongge Cave, China. Earth Planet. Sci. Lett. 233 (1–2), 71–86.

Fei, S., Weislogel, A., Sharma, S., Mullenex, A., Knight, E., Sun, G., 2013. Evolution of the Mesozoic Qamdo (Changdu) Basin, Eastern Tibet: linkages between sedimentation, climate, and regional tectonics. AAPG Annual Convention and Exhibition, Pittsburgh, Pennsylvania, May 19–22.

Gan, X., Li, H., Sun, D., Jin, W., Zhao, F., 1995. A geochronological study on early Proterozoic granitic rocks, southwestern Zhejiang. Acta Petrol. Mineral. 14, 1–8 (in Chinese).

Gao, S., Ling, W., Qiu, Y., Lian, Z., Hartmann, G., Simon, K., 1999. Contrasting geochemical and Sm–Nd isotopic compositions of Archean metasediments from the Kongling high-grade terrain of the Yangtze craton: evidence for cratonic evolution and redistribution of REE during crustal anatexis. Geochim. Cosmochim. Acta 63, 2071–2088.

Garzanti, E., Ando, S., Vezzoli, G., 2009. Grain-size dependence of sediment composition and environmental bias in provenance studies. Earth Planet. Sci. Lett. 277, 422–432.

Giosan, L., Clift, P.D., Macklin, M.G., Fuller, D.Q., Constantinescu, S., Durcan, J.A., Stevens, T., Duller, G.A.T., Tabrez, A., Adhikari, R., Gangal, K., Alizai, A., Filip, F., VanLaningham, S., Syvitski, J.P.M., 2012. Fluvial landscapes of the Harappan civilization. Proc. Natl. Acad. Sci. 109 (26), 1688–1694.

Granet, M., Chabaux, F., Stille, P., France-Lanord, C., Pelt, E., 2007. Time-scales of sedimentary transfer and weathering processes from U-series nuclides: clues from the Himalayan rivers. Earth Planet. Sci. Lett. 261 (3–4), 389–406.

Granet, M., Chabaux, F., Stille, P., Dosseto, A., France-Lanord, C., Blaes, E., 2010. U-series disequilibria in suspended river sediments and implication for sediment transfer time in alluvial plains: the case of the Himalayan rivers. Geochim. Cosmochim. Acta 74, 2851–2865.

Griffin, W.L., Belousova, E.A., Shee, S.R., Pearson, N.J., O'Reilly, S.Y., 2004. Archean crustal evolution in the northern Yilgarn Craton: U–Pb and Hf-isotope evidence from detrital zircons. Precambrian Res. 131 (3–4), 231–282.

He, M., Zheng, H., Clift, P.D., 2013a. Zircon U–Pb geochronology and Hf isotope data from the Yangtze River sands: implications for major magmatic events and crustal evolution in Central China. Chem. Geol. 360–361, 186–203.

He, M., Zheng, H., Huang, X., Jia, J., Li, L., 2013b. Yangtze River sediments from source to sink traced with clay mineralogy. J. Asian Earth Sci. 69 (5), 60–69.

He, M., Zheng, H., Jia, J., 2013c. Detrital zircon U–Pb dating and Hf isotope of modern sediments in the Yangtze River: implications for the sediment provenance. Quat. Sci. 33 (4), 656–670.

He, S., Li, R., Wang, C., Gu, P., Yu, F., Shi, C., Zha, X., 2013d. Research on the formation age of Ningduo Rock Group in the Changdu Block: evidence for the existence of basement in the North Qiangtang. Earth Sci. Front. 20 (5), 15–24.

Hoang, L.V., Clift, P.D., Mark, D., Zheng, H., Tan, M.T., 2010. Ar–Ar muscovite dating as a constraint on sediment provenance and erosion processes in the Red and Yangtze River systems, SE Asia. Earth Planet. Sci. Lett. 295, 379–389.

Hodges, K., Ruhl, K., Wobus, C., Boyce, J., 2005. Detrital mineral thermochronology in active fluvial systems and the evolution of modern orogenic landscapes. Geochim. Cosmochim. Acta 69 (10), A296-A296.

Hu, X.J., Xu, J.K., Tong, C.X., Chen, C.H., 1991. The Precambrian geology of Southwestern Zhejiang province. Precambrian Geology, 5. Geological Publishing House, Beijing, China, p. 278.

Hu, J., Meng, Q., Shi, Y., Qu, H., 2005. SHRIMP U–Pb dating of zircons from granitoid bodies in the Songpan–Ganzi terrane and its implications. Acta Petrol. Sin. 21 (3), 867–880.
Hu, D., Clift, P.D., Böning, P., Hannigan, R., Hillier, S., Blusztajn, J., Wang, S., Fuller, D.Q., 2013. Holocene evolution in weathering and erosion patterns in the Pearl River delta. Geochem. Geophys. Geosyst. 14.
Huber, M., Goldner, A., 2012. Eocene monsoons. J. Asian Earth Sci. 44, 3–23.
Huntington, K.W., Hodges, K.V., 2006. A comparative study of detrital mineral and bedrock age-elevation methods for estimating erosion rates. J. Geophys. Res. 111 (F3), 11.
Jackson, S.E., Pearson, N.J., Griffin, W.L., Belousova, E.A., 2004. The application of laser ablation-inductively coupled plasma-mass spectrometry (LA-ICP-MS) to in situ U–Pb zircon geochronology. Chem. Geol. 211, 47–69.
Jia, J., Zheng, H., Tong, H., Wu, F., Yang, S., Wang, K., He, M., 2010. Detrital zircon U–Pb ages of late Cenozoic sediments from the Yangtze delta: implication for the evolution of the Yangtze River. Chin. Sci. Bull. 55 (4–5), 350–358.
Kirby, E., Whipple, K.X., 2012. Expression of active tectonics in erosional landscapes. J. Struct. Geol. 44, 54–75.
Lan, Z.W., Chen, Y.L., Su, B.X., Liu, F., Zhang, H.F., 2006. The origin of sandstones from the Songpan–Ganzi Basin, Sichuan, China: evidence from SHRIMP U–Pb dating of clastic zircons. Acta Sedimentol. Sin. 24, 321–332 (in Chinese).
Li, X.Z., Dodson, J., Zhou, X.Y., Zhang, H.B., 2007. Early cultivated wheat and broadening of agriculture in Neolithic China. The Holocene 17 (5), 555–560.
Li, W.-X., Li, X.-H., Li, Z.-X., Lou, F.-S., 2008. Obduction-type granites within the NE Jiangxi Ophiolite: implications for the final amalgamation between the Yangtze and Cathaysia Blocks. Gondwana Res. 13 (3), 288–301.
Li, X.-H., Li, W.-X., Li, Z.-X., Lo, C.-H., Wang, J., Ye, M.-F., Yang, Y.-H., 2009. Amalgamation between the Yangtze and Cathaysia Blocks in South China: constraints from SHRIMP U–Pb zircon ages, geochemistry and Nd–Hf isotopes of the Shuangxiwu volcanic rocks. Precambrian Res. 174 (1–2), 117–128.
Li, N., Chen, Y.J., Pirajno, F., Gong, H.J., Mao, S.D., Ni, Z.Y., 2012. LA-ICP-MS zircon U–Pb dating, trace element and Hf isotope geochemistry of the Heyu granite batholith, eastern Qinling, central China: implications for Mesozoic tectono-magmatic evolution. Lithos 142, 34–47.
Liu, S., Zhang, G., 1999. Process of rifting and collision along plate margins of the Qinling orogenic belt and its geodynamics. Acta Geol. Sin. 73 (3), 275–287 (in Chinese).
Ludwig, K., 2003. Isoplot 3.0. 4. Berkeley Geochronology Center.
Lupker, M., France-Lanord, C., Galy, V., Lave, J., Gaillardet, J., Gajured, A.P., Guilmette, C., Rahman, M., Singh, S.K., Sinha, R., 2012. Predominant floodplain over mountain weathering of Himalayan sediments (Ganga basin). Geochim. Cosmochim. Acta 84, 410–432.
Ma, X., Wu, D., 1987. Cenozoic extensional tectonics in China. Tectonophysics 133 (3–4), 243–255.
Milliman, J.D., Syvitski, J.P.M., 1992. Geomorphic/tectonic control of sediment discharge to the ocean; the importance of small mountainous rivers. J. Geol. 100, 525–544.
Molnar, P., England, P., Martinod, J., 1993. Mantle dynamics, uplift of the Tibetan Plateau, and the Indian monsoon. Rev. Geophys. 31 (4), 357–396.
Montgomery, D.R., 2007. Dirt: The Erosion of Civilizations. University of California Press, Berkeley, p. 285.
Ouimet, W.B., Whipple, K.X., Granger, D.E., 2009. Beyond threshold hillslopes: channel adjustment to base-level fall in tectonically active mountain ranges. Geology 37 (7), 579–582.
Prell, W.L., Kutzbach, J.E., 1992. Sensitivity of the Indian Monsoon to forcing parameters and implications for its evolution. Nature 360 (6405), 647–652.
Pubellier, M., Chamot-Rooke, N., Ego, F., Guezou, J.C., Konstantinovskaya, E., Rabaute, A., Ringenbach, J.C., 2008. Structural map of Eastern Eurasia. Commission for the Geological Map of the World.
Qin, J.F., Lai, S.C., Grapes, R., Diwu, C.R., Ju, Y.J., Li, Y.F., 2009. Geochemical evidence for origin of magma mixing for the Triassic monzonitic granite and its enclaves at Mishuling in the Qinling orogen (central China). Lithos 112 (3–4), 259–276.
Raymo, M.E., Ruddiman, W.F., 1992. Tectonic forcing of Late Cenozoic climate. Nature 359 (6391), 117–122.
Reid, A., Wilson, C.J.L., Shun, L., 2007. Mesozoic plutons of the Yidun Arc, SW China: U/Pb geochronology and Hf isotopic signature. Ore Geol. Rev. 31, 88–106.
Ryan, W.B.F., Carbotte, S.M., Coplan, J.O., O'Hara, S., Melkonian, A., Arko, R., Weissel, R.A., Ferrini, V., Goodwillie, A., Nitsche, F., Bonczkowski, J., Zemsky, R., 2009. Global Multi-Resolution Topography synthesis. Geochem. Geophys. Geosyst. 10 (Q03014).
Sun, W.H., Zhou, M.F., Gao, J.F., Yang, Y.H., Zhao, X.F., Zhao, J.H., 2009. Detrital zircon U–Pb geochronological and Lu–Hf isotopic constraints on the Precambrian magmatic and crustal evolution of the western Yangtze Block, SW China. Precambrian Res. 172, 99–126.
Syvitski, J.P.M., Kettner, A.J., 2011. Sediment flux and the Anthropocene. Philos. Trans. R. Soc. Lond. Ser. A: Math. Phys. Sci. 369, 957–975.
Syvitski, J.P.M., Kettner, A.J., Green, P., 2005. Impact of humans on the flux of terrestrial sediment to the global coastal ocean. Science 308, 376–380.
Vermeesch, P., 2004. How many grains are needed for a provenance study? Earth Planet. Sci. Lett. 224, 351–441.
Vermeesch, P., 2012. On the visualisation of detrital age distributions. Chem. Geol. 312–313, 190–194.
Wan, Y., Liu, D., Xu, M., 2007. SHRIMP U–Pb zircon geochronology and geochemistry of metavolcanic and metasedimentary rocks in Northwestern Fujian, Cathaysia block, China: tectonic implications and the need to redefine lithostratigraphic units. Tectonic Evol. China Adjacent Crustal Fragm. 12 (1–2), 166–183.
Wang, Y.J., Cheng, H., Edwards, R.L., An, Z.S., Wu, J.Y., Shen, C.-C., Dorale, J.A., 2001. A high-resolution absolute-dated late Pleistocene Monsoon record from Hulu Cave, China. Science 294, 2345–2348.
Wang, X.-L., Zhou, J.-C., Griffin, W.L., Wang, R.-C., Qiu, J.-S., O'Reilly, S.Y., Xu, X., Liu, X.-M., Zhang, G.-L., 2007. Detrital zircon geochronology of Precambrian basement sequences in the Jiangnan orogen: dating the assembly of the Yangtze and Cathaysia Blocks. Precambrian Res. 159 (1–2), 117–131.
Wang, T., Wang, X., Tian, W., Zhang, C., Li, W., Li, S., 2009. North Qinling Paleozoic granite associations and their variation in space and time: implications for orogenic processes in the orogens of central China Science in China Series D. Earth Sci. 52 (9), 1359–1384.
Wang, L.-J., Griffin, W.L., Yu, J.-H., O'Reilly, S.Y., 2010. Precambrian crustal evolution of the Yangtze Block tracked by detrital zircons from Neoproterozoic sedimentary rocks. Precambrian Res. 177 (1–2), 131–144.
Wang, L.J., Griffin, W.L., Yu, J.H., O'Reilly,, S.Y., 2012. U–Pb and Lu–Hf isotopes in detrital zircon from Neoproterozoic sedimentary rocks in the northern Yangtze block: implications for Precambrian crustal evolution. Gondwana Res. 23 (4), 1261–1272.
Wei, Q., Li, D., Wang, G., Zheng, J., 2007. Zircon SHRIMP U–Pb dating and geochemical characteristics of Chabaoma Formation volcanic rocks in northern Tibetan plateau and its petrogenesis. Acta Petrol. Sin. 23 (11), 2727–2736.
Weislogel, A.L., Graham, S.A., Chang, E.Z., Wooden, J.L., Gehrels, G.E., Yang, H.S., 2006. Detrital zircon provenance of the Late Triassic Songpan–Ganzi complex: sedimentary record of collision of the North and South China blocks. Geology 34 (2), 97–100.
Weisskopf, A.R., 2010. Vegetation, agriculture and social change in late Neolithic China: a phytolith study. Ph.D. Thesis University College London, p. 428.
Whitehead, J., Clift, P.D., 2009. Continent elevation, mountains, erosion and freeboard. J. Geophys. Res. 114.
Wittmann, H., von Blanckenburg, F., Maurice, L., Guyot, J.-L., Filizola, N., Kubik, P.W., 2011. Sediment production and delivery in the Amazon River basin quantified by in situ-produced cosmogenic nuclides and recent river loads. Geol. Soc. Am. Bull. 123 (5/6), 934–950.
Wobus, C.W., Whipple, K.X., Hodges, K.V., 2006. Neotectonics of the central Nepalese Himalaya; constraints from geomorphology, detrital $^{40}Ar/^{39}Ar$ thermochronology, and thermal modeling. Tectonics 25 (TC4011).
World Resources Institute, 2003. Yangtze - AS29, Watersheds of the World.
Wu, Z., Ye, P., Hu, D., Zhang, W., Zhou, C., 2007. U–Pb isotopic dating of zircons from porphyry granite of the Fenghuoshan Mts., northern Tibetan Plateau and its geological significance. Geoscience 21 (3), 435–442.
Wu, L., Li, F., Zhu, C., Li, L., Li, B., 2012. Holocene environmental change and archaeology, Yangtze River Valley, China: review and prospects. Geosci. Front. 3 (6), 875–892.
Xia, Y., Xu, X., Zhu, K., 2012. Paleoproterozoic S- and A-type granites in southwestern Zhejiang: magmatism, metamorphism and implications for the crustal evolution of the Cathaysia basement. Precambrian Res. 216–219, 177–207.
Xu, J.F., Hou, L., Wang, Z., 1992. Orogenic Process of the Songpan–Garze Orogenic Belt of China (in Chinese with English abstract). Geological Publishing House, p. 190.
Xu, Y.G., Luo, Z.Y., Huang, X.L., 2008. Zircon U–Pb and Hf isotope constraints on crustal melting associated with the Emeishan mantle plume. Geochim. Cosmochim. Acta 72, 3084–3104.
Yang, S., Jung, H.-S., Li, C., 2004a. Two unique weathering regimes in the Changjiang and Huanghe drainage basins: geochemical evidence from river sediments. Sediment. Geol. 164, 19–34.
Yang, S., Jung, H.-S., Li, C., 2004b. Two unique weathering regimes in the Changjiang and Huanghe drainage basins: geochemical evidence from river sediments. Sediment. Geol. 164 (1–2), 19–34.
Yang, S., Wang, Z., Guo, Y., Li, C., Cai, J., 2009. Heavy mineral compositions of the Changjiang (Yangtze River) sediments and their provenance-tracing implication. J. Asian Earth Sci. 35 (1), 56–65.
Yang, Y., Yuan, D., Cheng, H., Zhang, M., Qin, J., Lin, Y., Zhu, X., Lawrence, E.R., 2010. Precise dating of abrupt shifts in the Asian Monsoon during the last deglaciation based on stalagmite data from Yamen Cave, Guizhou Province, China. Sci. China B 53, 633–641.
Yang, S., Zhang, F., Wang, Z., 2012. Grain size distribution and age population of detrital zircons from the Changjiang (Yangtze) River system, China. Chem. Geol. 296–297, 26–38.
Yao, J.L., Shu, L.S., Santosh, M., 2011. Detrital zircon U–Pb geochronology, Hf-isotopes and geochemistry—New clues for the Precambrian crustal evolution of Cathaysia Block, South China. Gondwana Res. 20 (2–3), 553–567.
Zhang, P., 2013. A review on active tectonics and deep crustal processes of the western Sichuan region, eastern margin of the Tibetan Plateau. Tectonophysics 584, 7–22.
Zhang, G., Cheng, S., Guo, A., Dong, Y., Lai, S., Yao, A., 2004. Mianlue paleo-suture on the southern margin of the Central Orogenic System in Qinling–Dabie—with a discussion of the assembly of the main part of the continent of China. Geol. Bull. China 23 (9–10), 846–853.
Zhang, H.-F., Zhang, L., Harris, N., Jin, L.-L., Yuan, H., 2006. U–Pb zircon ages, geochemical and isotopic compositions of granitoids in Songpan–Garze fold belt, eastern Tibetan Plateau: constraints on petrogenesis and tectonic evolution of the basement. Contrib. Mineral. Petrol. 152 (1), 75–88.
Zhang, H., Bevan, A., Fuller, D., Fang, Y., 2010. Archaeobotanical and GIS-based approaches to prehistoric agriculture in the Upper Ying Valley, Henan, China. J. Archaeol. Sci. 37 (7), 1480–1489.
Zhao, Z.F., Zheng, Y.F., Wei, C.S., Chen, F.K., Liu, X.M., Wu, F.Y., 2008. Zircon U–Pb ages, Hf and O isotopes constrain the crustal architecture of the ultrahigh-pressure Dabie orogen in China. Chem. Geol. 253, 222–242.
Zhou, D., Garanham, S.A., 1993. Songpan–Garze Rriassic complex as a remnant ocean basin along diachronous collision orogen, central China. Geol. Soc. Am. Abstr. Programs 25, A118.